2019-08-01

Improvements to Sound Power Measurements for Large, Extended Sources in Semi-Reverberant Rooms Using Generalized Energy Density

Travis Nathan Hoyt
Brigham Young University

Improvements to Sound Power Measurements for Large, Extended Sources in Semi-Reverberant Rooms Using Generalized Energy Density

Travis Nathan Hoyt

A thesis submitted to the faculty of
Brigham Young University
in partial fulfillment of the requirements for the degree of

Master of Science

Scott D. Sommerfeldt, Chair
Timothy W. Leishman
Jonathan D. Blotter

Department of Physics and Astronomy

Brigham Young University

ABSTRACT

Improvements to Sound Power Measurements for Large, Distributed Sources in Semi-Reverberant Rooms Using Generalized Energy Density

Travis Nathan Hoyt
Department of Physics and Astronomy, BYU
Master of Science

Sound power measurements of acoustic sources are typically performed in anechoic or reverberation chambers using acoustic pressure according to international standards. The anechoic chamber creates a free-field environment where the sound power is estimated from the squared pressure integrated over some enveloping surface. The reverberation chamber produces diffuse-field conditions, where sound power is proportional to the spatially averaged squared pressure. In semi-reverberant environments, the direct and reverberant energies each contribute to the total measured field. If the kinetic and potential components of acoustic energy density are weighted appropriately, the spatial variation of the field can be significantly reduced compared to squared pressure. This generalized energy density allows an adaptation of the sound power formulation by Hopkins and Stryker to be used to make an efficient and accurate in situ sound power estimate of a noise source in a non-ideal acoustical environment. Since generalized energy density optimizes the spatial uniformity of the field, fewer measurement positions are needed compared to traditional standards. However, this method breaks down for sources that are large and extended in nature and considerably underestimates the sound power. This thesis explores the practical limits of this method related to the sound power underestimation. It also seeks to understand the special considerations necessary to achieve accurate, survey-grade sound power data of large, extended noise sources through a laboratory study of custom extended and compact sources. A modified method to accurately and efficiently measure the sound power of large, extended sources is proposed with results.

Keywords: sound power, generalized energy density, semi-reverberant enclosure

ACKNOWLEDGEMENTS

I would like to thank my advisor, Dr. Scott Sommerfeldt, for his continued support and guidance throughout this project. I thank Dr. Timothy Leishman for inspiring me to chase my dreams no matter the cost and for encouraging me to pursue a graduate degree. I thank Dr. Blotter for his steady support and consultation related to this project. I also wish to express my gratitude for the entire BYU Acoustics faculty who have mentored me and guided me in research and coursework. I also thank my peers, many of whom have directly contributed to my research by taking data and helping assemble and disassemble experimental setups. I am grateful for Danny Marquez and Zachary Jensen for their mentorship and well-documented research that laid the groundwork for this specific project. I give thanks to David Copley and the research sponsor for making this project possible and for continuing to pursue this research even when results were discouraging for a time. Most of all, I thank my wife, Kaitlyn, for her unwavering love and devotion to me, even when circumstances made the task of completing this research and thesis seem unachievable.

Table of Contents

List of Tables

List of Figures

Chapter 1

Introduction

Sound is vibration that propagates as an audible pressure wave through a medium. For humans, sound is the reception of such waves and their perception by the brain. Noise, in the realm of acoustics, is typically defined as unwanted sound. To quantify the performance of acoustic noise sources, acousticians often conduct sound power measurements of said sources. Sound power is a useful metric for describing the total sound radiated from a source, since unlike pressure, it does not depend on distance from the source. Sound power is generally estimated in qualified reverberation or anechoic chambers, using microphones to measure pressure and calculating the sound power according to specific ISO, ANSI, and other internationally accepted standards.

This thesis proposes a simplified method for sound power estimation in semi-reverberant rooms using generalized energy density. It also clarifies the limitations of previous work, and introduces improvements based on previous inaccuracies encountered when measuring large, extended noise sources.

1.1 Previous Work

The sound power of noise sources has been a long-standing subject of interest of acousticians, engineers, and end users. The development of products that radiate high levels of sound often includes design to meet noise criteria, or to match or surpass the noise-mitigation techniques of competitors. In order to design around specific criteria, it is critical to evaluate the sound power of a source. While radiated sound pressure level has historically been a popular data point for quantifying noise, the measurements are entirely dependent on distance and direction from the source to the microphone, and the acoustical environment where the measurement was performed. Today, sound power is often the preferred metric, since it is a global quantity that doesn't depend on distance, direction, or room acoustics, and its measurement methods in a laboratory setting are well documented by various international standards.

Sound power is the time-averaged acoustic energy flux (through some enveloping surface) per unit time produced by a noise source. It is difficult to directly measure sound power, since it requires knowledge of the entire acoustic field. Instead, acoustic pressure measurements are sampled throughout the field in highly specialized acoustical environments to estimate its value. These particular acoustical environments are typically extreme cases, with walls that are either very rigid and thus acoustically reflective, known as reverberation chambers, or extremely absorptive, known as anechoic chambers.

In a reverberation chamber, sound waves propagate from the source to the walls, where the waves are then reflected multiple times before decaying due to atmospheric absorption and

losses inherent in the room. This allows for the assumption of a diffuse-field environment. A diffuse field is characterized by an equal distribution of energy density throughout the room, with the flow of energy density indifferent of direction. This means that at any point, there is an equal probability of simultaneous sound arriving from any direction. In such a field, the sound power is directly proportional to the spatially averaged energy density, which is proportional to the spatially averaged squared pressure, which can be measured with multiple microphone measurements. ISO 3741 details the procedure for performing these diffuse-field measurements.[1] The standard dictates that the pressure must be sampled in at least six locations simultaneously, with specification for the minimum separation distances between microphones and distances between microphones, the source, and chamber surfaces. It is also often required to take measurements with the source in different locations. Depending on the size of the chamber, it can be difficult to meet all of these requirements. It should be noted that even qualified reverberation chambers only approximate a diffuse field, and the spatial pressure response can vary considerably. Absorption in the room also affects the spatial variance in pressure.

In an anechoic chamber, the walls are typically comprised of several feet of absorptive wedges that absorb the incident sound waves by dissipating the kinetic energy of the air particles in the propagating wave to heat. A qualified anechoic chamber absorbs 99% of all incident acoustic energy above its cutoff frequency.[2] The virtual absence of reverberant energy allows for the assumption of a free-field condition, where only direct sound pressure from the source propagates and the intensity decays according to the inverse square law. In a free field, the sound power of a source is proportional to the mean-square acoustic pressure integrated over a

continuous (hypothetical) surface enveloping the source. This allows for the approximation of the acoustic energy flux through the surface, which is proportional to the sound power of the source. The ISO 3744 and 3745 standards detail the specific methods and measurement procedures for estimating the sound power via sound pressure measurements over measurement spheres or hemispheres.[2,3] These can be particularly cumbersome, because the standards require over 20 measurement positions to sufficiently sample the radiating field along the hypothetical surface. In cases where high-accuracy and high-frequency information is critical, thousands of measurement points could be needed.[4]

In semi-reverberant environments, a source radiates into an acoustic space and its direct energy spreads according to the inverse-square law until it meets a boundary. Depending on the boundary material involved, a certain amount of energy is then absorbed, and the remainder is reflected. This reflected energy contributes to reverberant energy. In rooms that are highly absorptive, the direct energy dominates the reverberant energy and has the most profound effect on the overall energy in the room. In these environments, the source behaves much as it would in a free field, with minimal contributions by reverberant energy at most locations in the total field. In rooms that are highly reflective, the opposite is true. The reverberant energy dominates the direct energy and has the overwhelming influence on the total energy at most locations. The characteristics of the room will thus dictate the overall energy in the room.

The locally averaged energy density reaches a steady-state condition when the rate of absorption in the room meets the running-time rate at which the source is emitting energy into the room. In such a condition, the energy density at any point is comprised of the direct energy

density, that which would be measured if the source were in a free field, and the reverberant energy density, which is assumed to be diffuse. Thus, the total field at any point is the aggregate of these direct and reverberant energies. This can make sound power estimation difficult, since both energies must be simultaneously considered together, but cannot readily be differentiated into their respective parts.

In the late 1940s, Hopkins and Stryker published an expression that describes the total energy density in terms of its direct and reverberant components.[5] This formulation, which will be referred to as the Hopkins-Stryker equation, is expressed as

$$\langle w_T(r,\theta_0,\phi_0)\rangle_{t,s} = \frac{\langle \Pi \rangle_t}{c}\left[\frac{\gamma(\theta_0,\phi_0)}{4\pi r^2} + \frac{4}{R}\right], \tag{1.1}$$

where $\langle w_T \rangle_{t,s}$ is the temporal and local spatially averaged total energy density (TED), $\langle \Pi \rangle_t$ is the time-averaged sound power of the device under test (DUT), γ is the far-field directivity factor of the DUT at some angle (θ_0, ϕ_0), r is the distance from the acoustic center of the DUT, c is the speed of sound, and R is the room constant, which is classically defined as $R = S\bar{\alpha}/1-\bar{\alpha}$, where S is the total surface area and $\bar{\alpha}$ is the mean absorption coefficient of the room. Here θ_0 represents the polar angle in the vertical plane and ϕ_0 represents the azimuthal angle defined in the horizontal plane. The TED is the sum of the spatially averaged potential energy density (PED) and kinetic energy density (KED). The first term in the square brackets in Eq. (1.1) is proportional to the direct energy density and is referred to in this thesis as the direct sound term.

The second term is proportional to the reverberant energy density, and is thus referred to as the reverberant sound term.

There are multiple methods for measuring the sound power of a source by applying the principles of direct and reverberant fields as described in the Hopkins-Stryker equation. For example, the ISO 3741 standard for sound power measurements in reverberation chambers exploits the expression by requiring a dominant reverberant field so that only the reverberant term is considered. Instead of local averaging, the standard requires multiple measurement positions, throughout the test environments.

Most rooms are neither sufficiently anechoic to assume a free field nor reverberant enough to be considered diffuse. For these nonideal, semi-reverberant acoustic spaces, other means must be utilized to achieve the estimated sound power. These methods rely on the Hopkins-Stryker equation, employing the established relationships between total energy density, room constant, directivity factor, and sound power. Each of the aforementioned means of sound power estimation rely on squared pressure measurements, which are proportional to the PED, but the Hopkins-Stryker equation relies on a local spatial average of the TED. The TED is considerably more spatially uniform than PED which makes it an advantageous quantity, since fewer spatial samples are needed to yield an appropriate representation of the field.[6]

In 2010, Xu et al. proposed generalized energy density (GED), which is essentially a "weighted" total energy density, whose PED and KED components are scaled by a constant. This was shown to produce even lower spatial variation than TED.[6]

In 2014, Marquez introduced a related two-point in situ method as a means for estimating the sound power of a noise source in a semi-reverberant space. This requires a reference directivity source with a known directivity factor and two GED measurements to empirically determine the room constant. Once that is known, two GED measurements of the DUT are taken at some angle within the semi-reverberant field. Simultaneous solution of two instances of the Hopkins-Stryker equation is then used to extract the estimated sound power and directivity factor of the source. With this method, the sound power of a loudspeaker was measured to acceptable accuracy in various semi-reverberant rooms, but the directivity factor and room constant results consistently diverged from predictions.[7]

In 2016, Jensen continued work on the two-point in situ method with substantial contributions to the methods of room constant measurements. He introduced a near-field correction term for the direct term for use with compact source measurements that could be approximated by a monopole. He also studied the effect of local averages to assess the spatial robustness of generalized energy density in practice and its effect on the method. His contributions to the two-point in situ method produced encouraging results. The sound power was shown to be successfully estimated for various compact noise sources such as vacuum cleaners, belt sanders, fans, and various loudspeakers. However, when the method was applied to a large complex industrial source, the method considerably underestimated the sound power of said source and yielded estimated directivity factors that were not physically viable.[8]

1.2 Motivation for Research

Since sound power measurements are becoming more common, research documenting measurement techniques in both ideal and nonideal acoustical environments should be clarified and scaled for many types of sources. While the estimation of sound power in ideal enclosures is relatively well known and documented in standards, methods for sound power estimation in non-ideal enclosures are much less understood. Identifying and addressing the limitations of previous research in this area could potentially lead to the development of novel measurement standards for these nonideal, semi-reverberant environments. These methods could be valuable to academia and industry, since the ability to make meaningful sound power measurements in semi-reverberant rooms reduces the need for costly measurement chambers and cumbersome techniques. Not only would they reduce the overall number of required measurement positions, but also the overall cost of measurements.

The developments and experimental validations performed by Marquez and Jensen on the two-point in situ method in semi-reverberant environments has demonstrated the capabilities of sound power estimation in semi-reverberant rooms using GED. However, they are unfortunately limited to compact sources. When applied to larger, extended sources that radiate with a more complex sound field, the method consistently underestimates the overall power of the DUT.[8] It was suspected that this was in part due to the violation of some or all of the underlying assumptions in the derivation of the Hopkins-Stryker equation. This is the primary motivation for the present research, since careful determination of the practical limits of the method, as well as

the development of any modifications that could allow the method to properly apply to large, extended sources, are acutely needed for many applications.

1.3 Objectives

The primary objective of this research was to address the shortcomings of the results of the two-point GED method when applied to large, extended sources and to modify it in such a way that allowed it to estimate the in situ sound power of large, extended industrial noise sources for survey-grade accuracy. This was accomplished through the following steps:

1. Carefully explore the assumptions and conditions built into the theory supporting the Hopkins-Stryker equation to identify if assumptions were violated when applied to large, complex sources.
2. Recreate a large complex source in a laboratory setting that produces results consistent with the underestimation seen in Jensen's work on large industrial noise sources in semi-reverberant environments.
3. Determine the root cause of the underestimation and explore options to enhance or otherwise alter the two-point method to allow estimation of large, distributed acoustic sources.
4. Identify the specific measurement conditions that provide acceptable results.
5. Develop a survey-grade (or better) measurement method that can properly estimate the sound power of large industrial noise sources in semi-reverberant enclosures.

Additional details surrounding these objectives will be presented in the remainder of this thesis.

1.4 Plan of Development

This introductory chapter has detailed the general background of the research problem, summarized previous work on related topics, outlined the motivations for and objectives of the research performed, and defined the scope of this thesis. The remainder of the thesis will be organized as follows. Chapter 2 will present the supporting theory of the two-point in situ method with critical clarifications of assumptions and limitations inherent in the theoretical development of the Hopkins-Stryker equation. Chapter 3 will detail the approach of experimental research to determine the conditions causing underestimation, and the experiments designed to further investigate the results. Chapter 4 will discuss the experimental results of the two-point method and their relevance to the research problem. Chapter 5 introduces a simplified method for making sound power measurements and provides results and limitations when applied to large, extended sources. Chapter 6 then summarizes the work performed and makes suggestions for future work related to this research. An appendix contains MATLAB codes related to this work.

Chapter 2

Theory

The theoretical developments involved in the formulation of the expressions relating sound power to energy density, such as in the Hopkins-Stryker equation, are acutely relevant to this research since it seeks to address any violations to the underlying theory, which may account for the sound power underestimation when measuring sources that are large and extended in nature. Therefore, the theoretical basis for relevant energy-based acoustics measurements will be discussed in detail, from the fundamentals of TED, the developments and advantages of GED, the Hopkins-Stryker equation and each of its parts, to the two-point in situ method.

2.1 Acoustic Energy Density

The time-averaged, discrete-point TED is the direct sum of PED and KED:

$$\langle w_T \rangle_t = \langle w_P \rangle_t + \langle w_K \rangle_t. \tag{2.1}$$

The expression for GED differs slightly from that of TED, namely[6]

$$\langle w_{G,\beta} \rangle_t = \beta \langle w_P \rangle_t + (1-\beta)\langle w_K \rangle_t \,, \tag{2.2}$$

where $\langle w_{G,\beta} \rangle_t$ is the time-averaged GED and β is the weighting factor. For a truly diffuse field, a weighting factor of $\beta = 0.25$ has been shown to minimize spatial variance.[6] The PED and KED are respectively defined as

$$\langle w_P \rangle_t = \frac{\langle p^2 \rangle_t}{2\rho_0 c^2} \tag{2.3}$$

and

$$\langle w_K \rangle_t = \frac{\rho_0}{2} \langle |\boldsymbol{u}|^2 \rangle_t, \tag{2.4}$$

where $\langle p^2 \rangle_t$ is the time-averaged squared pressure, ρ_0 is the density of air, and $|\boldsymbol{u}|$ is the vector magnitude of the particle velocity.

The values of PED, KED, and TED can be achieved with various values of β:

$$\langle w_{G,1} \rangle_t = \langle w_P \rangle_t; \ \beta = 1, \tag{2.5a}$$

$$\langle w_{G,0} \rangle_t = \langle w_K \rangle_t; \ \beta = 0, \tag{2.5b}$$

$$\langle w_{G,1/2} \rangle_t = \frac{\langle w_T \rangle_t}{2}; \ \beta = \frac{1}{2}. \tag{2.5c}$$

If the plane-wave assumption is applied, $\langle w_P \rangle_{t,s} = \langle w_K \rangle_{t,s}$, then for any value of β the expression for GED becomes $\langle w_{G,\beta} \rangle_{t,s} = \langle w_P \rangle_{t,s} = \langle w_K \rangle_{t,s} = \langle w_T \rangle_{t,s}/2$, which allows Eq. (1.1) to be expressed as its GED counterpart

$$\langle w_{G,\beta} \rangle_{t,s} = \frac{\langle \Pi \rangle_t}{2c} \left[\frac{\gamma(\theta_0, \phi_0)}{4\pi r^2} + \frac{4}{R} \right], \tag{2.6}$$

which is the Hopkins-Stryker equation in terms of GED. Note that the expressions for TED, PED, KED, and GED in Eqs. (2.1) through (2.5) describe the time-averaged but not spatially

averaged energy density. However, the Hopkins-Stryker equation is defined in terms of the local spatially and temporally averaged energy density. The assumption is made that since GED is much more spatially uniform than TED, its value at a point and its local spatial average about that point are similar enough to be considered identical in this context.

2.2 The Hopkins-Stryker Equation

The instance of the Hopkins-Stryker equation to be used in this thesis is the GED variant, as expressed in Eq. (2.6). It describes the relative contributions to the total GED of the direct energy density

$$\langle w_{G,\beta,D} \rangle_{t,s} = \frac{\langle \Pi \rangle_t}{2c} \frac{\gamma(\theta_0, \phi_0)}{4\pi r^2} \tag{2.7}$$

and reverberant energy density

$$\langle w_{G,\beta,R} \rangle_{t,s} = \frac{\langle \Pi \rangle_t}{2c} \frac{4}{R}. \tag{2.8}$$

The direct term dominates the expression near the source, since it dictates the field before reaching the point where spherical spreading is overpowered by the reverberant field. As the distance between the source and field point increases, the reverberant term begins to dominate the expression since the energy density reaches the aforementioned steady state that is dependent on the acoustics of the room. At some distance, the contributions of the direct [Eq. (2.7)] and reverberant [Eq. (2.8)] energy density fields will be equal. This is referred to as the critical distance, and is defined as

$$r_c = \sqrt{\frac{\gamma(\theta_0, \phi_0)R}{16\pi}}. \tag{2.9}$$

The general relationship between the direct and reverberant energy densities with respect to the aggregate energy density as described by the Hopkins-Stryker equation is illustrated graphically in Fig. 2.1. Here the composite energy density components for a hypothetical source in a room are calculated relative to the reverberant energy density, which is dictated by the room constant.

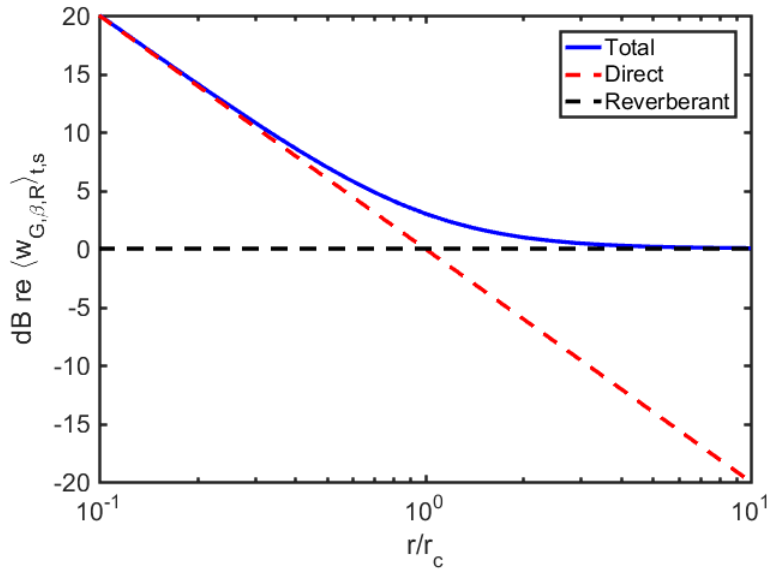

Fig 2.1. The total energy density level of a simple source per the Hopkins-Stryker equation is the energetic sum of the direct-field and reverberant-field levels.

2.3 The Reverberant Energy Density Term

The reverberant term [Eq. (2.8)] is characterized by the quantity $4/R$. This follows from the assumption of a diffuse reverberant field, which is defined as having uniform local spatially averaged energy density throughout the field. Since the reverberant field is dictated by the room

absorption, which is constant, it would follow that the steady-state reverberant energy would be constant. As the distance from the source increases, it will converge to a single value that is independent of position. The diffuse-field assumption can be violated in rooms with complex or irregular geometries, nonuniform distribution of absorbing surfaces, excessive absorption, or features with abnormal scattering. The volume and geometry of a room directly affect the strength of the diffuse-field assumption. In corridors or other rooms where one dimension is significantly larger than the others, the energy density flow is emphasized in the direction away from the source, rather than being randomly distributed about the measurement point. Rooms with high absorption dissipate the reverberant energy to a point where there is not enough reflected energy to be considered diffuse. These types of rooms, in addition to especially voluminous rooms, can suffer from a phenomenon of reverberant energy decaying with increased distance.[9]

The 4 in the numerator of Eq. (2.8) comes from the expression for the mean free path, which is the average distance a sound wave travels before encountering a boundary in an enclosed field. For a diffuse field in a nominally cubic room, the mean free path is expressed as[10]

$$L = \frac{4V}{S}, \tag{2.10}$$

where V is the room volume and S is the room surface area.

The room constant R is a frequency-dependent value that is a function of the average absorption, $\bar{\alpha}$, in the room and its surface area. It is a straightforward means of quantifying the sound absorption in a room. There is a considerable amount of discussion about the validity of

the traditional expression for the room constant in the literature,[10,11,12] but is defined by Hopkins and Stryker as[5]

$$R = \frac{S\bar{\alpha}}{1-\bar{\alpha}} \ . \tag{2.11}$$

2.4 The Direct Energy Density Term

The direct-term expression in Eq. (2.7) describes the direct energy density due to radiation at some point a distance r from the source, where the inverse-square law for intensity is observed. It assumes that measurements are made in the direct far field, which is characterized by spherical spreading. In this case, the PED and KED are equal. In practice, it can be difficult to estimate the distance needed to achieve the direct far field, since the reverberant field begins to dominate as the distance from the source increases. Beranek suggests that the direct far field begins at least 1/3 of a wavelength from a compact source.[10]

The directivity factor is included in the numerator of Eq. (2.7) to account for non-uniform angular dependence in radiation. Beranek defines the directivity factor as the ratio of radiated intensity at some angle to the intensity at the same point due to a monopole radiating the same sound power,[10] which can be expressed as

$$\gamma(\theta_0, \phi_0) = \frac{\langle I(\theta_0, \phi_0)\rangle_t}{\langle I_m\rangle_t}. \tag{2.12}$$

Hopkins and Stryker assumed that this directivity factor had constant values of 1, 2, or 4, depending on whether the source was in free space, near a reflecting plane, or in a dihedral

corner, respectively. Although these assumed values were treated as constants, in practice they vary with angle and frequency. The directivity factor will also change over distance, since the near-field behavior varies significantly from far-field characteristics. In this work, the far-field directivity factor is assumed.

For limited r, within the dimensions of many rooms, the direct term only describes the direct energy density of a compact source spherically radiating in the direct far field. The direct energy density of a large, extended noise source, will not be well described by this expression.

2.5 The Two-Point In Situ Method

The two-point in situ method, introduced by Marquez, allows for a straightforward estimation of the sound power using two sets of two GED measurements.[7] This method directly measures the room constant using a reference directivity source, rather than estimating it using the other methods. The room constant is then used in a variation of the Hopkins-Stryker equation to solve for the estimated sound power of the DUT.

The reference directivity source, whose directivity factor $\gamma_{ref}(\theta_0, \phi_0)$ has been previously measured, is measured in the room along a line at some angle from the source at two distinct positions r_1 and r_2. This allows for two equations,

$$\langle w_{1,G,\beta} \rangle_{t,s} = \frac{\langle \Pi \rangle_{t,ref}}{2c} \left[\frac{\gamma_{ref}(\theta_0, \phi_0)}{4\pi {r_1}^2} + \frac{4}{R} \right] \tag{2.13a}$$

and

$$\langle w_{2,G,\beta}\rangle_{t,s} = \frac{\langle \Pi\rangle_{t,ref}}{2c}\left[\frac{\gamma_{ref}(\theta_0,\phi_0)}{4\pi {r_2}^2} + \frac{4}{R}\right]. \tag{2.13b}$$

Ideally, one of these positions is between the source and critical distance, while the other is beyond the critical distance, to sample the field where each term is dominant in the expression.[7] The two expressions [Eq. (2.13a) and Eq. (2.13b)] contain two unknowns: the reference source power (although this is often known since directivity measurement data can be used to calculate it via ISO 3745) and the room constant. The room constant is then solved for using

$$R = \frac{16\pi\left(\frac{\langle w_{2,G,\beta}\rangle_{t,s}}{\langle w_{1,G,\beta}\rangle_{t,s}} - 1\right)}{\gamma_{ref}(\theta_0,\phi_0)\left(\frac{1}{r_2^2} - \frac{\langle w_{2,G,\beta}\rangle_{t,s}}{\langle w_{1,G,\beta}\rangle_{t,s} r_1^2}\right)}. \tag{2.14}$$

With the room constant measured, the DUT is then measured in the room with two more GED measurements at positions r_3 and r_4:

$$\langle w_{3,G,\beta}\rangle_{t,s} = \frac{\langle \Pi\rangle_{t,DUT}}{2c}\left[\frac{\gamma_{DUT}(\theta_0',\phi_0')}{4\pi {r_3}^2} + \frac{4}{R}\right], \tag{2.15a}$$

and

$$\langle w_{4,G,\beta}\rangle_{t,s} = \frac{\langle \Pi\rangle_{t,DUT}}{2c}\left[\frac{\gamma_{DUT}(\theta_0',\phi_0')}{4\pi {r_4}^2} + \frac{4}{R}\right]. \tag{2.15b}$$

These may be along a line at any angle from the DUT, indicated by (θ_0', ϕ_0'). The directivity factor of the DUT at this angle and its sound power are then solved for using

$$\gamma_{DUT}(\theta_0', \phi_0') = \frac{16\pi\left(\frac{\langle w_{4,G,\beta}\rangle_{t,s}}{\langle w_{3,G,\beta}\rangle_{t,s}} - 1\right)}{R\left[\frac{1}{r_4^2} - \frac{\langle w_{4,G,\beta}\rangle_{t,s}}{\langle w_{3,G,\beta}\rangle_{t,s} r_3^2}\right]} \tag{2.16}$$

and

$$\langle \Pi_{DUT}\rangle_t = \frac{2\langle w_{3,G,\beta}\rangle_{t,s} c}{\left(\frac{\gamma_{DUT}(\theta_0', \phi_0')}{4\pi {r_3}^2} + \frac{4}{R}\right)}, \tag{2.17}$$

respectively.

2.6 Discussion

The assumptions in the Hopkins-Stryker equation require that measurements be taken in the direct far field of a source, where the plane wave assumption can be reasonably made. Depending on the room, this can be impossible due to room dimensions that are smaller than the required far field, r, or the critical distance, since two-point method measurements are to be made on either side of the critical distance. The size of the source can complicate the application of the Hopkins-Stryker equation, since large, extended sources have direct far fields that are much farther from the source than those of compact sources. In smaller rooms, it may be impossible to reach the direct far field, where the assumptions in the underlying theory for the direct term are applicable. Furthermore, the direct term assumes spherical spreading, which may not accurately describe the radiation near larger, complex sources.

The diffuse field assumption for the reverberant term can be compromised by excessive absorption in the room, or by a nonuniform distribution of absorbing surfaces. This is known to

introduce error into the sound power estimation, since reverberant field theory relies on uniform boundaries and well-distributed absorption in order to reasonably assume a diffuse-field condition.

Point generalized energy density measurements are also being considered in place of local spatial averages, which rely on the assumption that the field is sufficiently uniform. The errors in sound power estimation associated with nonuniform energy density increase with room absorption and at field points that are in the near field of a source.

Chapter 3

Experiment Design

One of the interesting findings of Jensen was that the two-point method produced sound power results consistent with ISO 3741 and ISO 3745 measurements for various compact sources, but diverged from ISO standard results for larger, more extended sources.[8] The two-point method allows for the simultaneous estimation of both the sound power and the directivity factor of the DUT. While the directivity factor may not be as interesting in some applications as the sound power data, results for the directivity factor seemed to be far from expected values for some sources.[7,8] Since the sound power results seemed to agree with results from standardized measurements, no further efforts were dedicated to the discrepancy. When the two-point method was applied to a large industrial source in a room, the sound power results estimated a power that was consistently 4 to 6 dB lower than that determined from standardized measurements.[8] In addition, the directivity factors estimated by the two-point method were often not physically viable.

This work aims to better understand the two-point method by investigating the direct term in more detail and carefully determining the practical limits of the method. To do so, multiple experiments were designed, constructed, and performed to acquire data that would lend additional insight related to the two-point method procedure and calculation.

First, it was necessary to create a source in a laboratory setting that was large and extended enough to cause the two-point method to underestimate the sound power in a manner similar to Jensen's measurements. Second, to remove a degree of freedom from the two-point method's final calculation in Eq. (2.7), two sources were constructed and their directivity factors were measured in the azimuthal and polar planes according to a variant of ISO 3745. The first source was a single 13 cm loudspeaker in a small box. The second was a line array of 16 of these 13 cm loudspeakers in a 2.34 meter long array. These measured directivity factors were then used instead of calculated ones in two-point measurements of these sources. The sound powers of these two sources were also measured according to ISO 3741.

3.1 Measurement of Energy Density

The acoustic energy density in this work was measured using a G.R.A.S. 50V-I-1 vector intensity probe, consisting of three orthogonal phase-matched pairs of microphones, whose pairs were indexed as 1-2, 3-4, and 5-6. These microphones were separated by a 25 mm spacer, whose spatial Nyquist frequency allows for a working frequency range of roughly 125 Hz to 5,500 Hz.[13] To measure the GED with a vector intensity probe consisting of microphones measuring pressure, the PED and KED are measured using a method offered by Pascal and Li that uses the

finite-difference method, the auto-spectrum, and the cross-spectrum of the probe microphone signals.[14] The PED is given by the expression

$$\text{PED} = \frac{1}{24\rho_0 c^2}\sum_{i=1}^{6} G_{ii} + \frac{1}{12\rho_0 c^2}[C_{21} + C_{43} + C_{65}] \tag{3.1}$$

and the KED is given by

$$\text{KED} = \frac{1}{2\rho_0 c^2 k^2 d^2}\sum_{i=1}^{6} G_{ii} - \frac{1}{\rho_0 c^2 k^2 d^2}[C_{21} + C_{43} + C_{65}], \tag{3.2}$$

where ρ_0 is the density of air, c is the speed of sound, k is the wavenumber, d is the microphone spacing, G_{ii} is the auto-spectrum of the ith microphone, and C_{ij} is the real part of the cross-spectrum between the ith and jth microphones, which are arranged opposite each other.

3.2 The Reference Directivity Source

The reference directivity source used for two-point method measurements (the same used by Jensen) was a 7.6 cm full-range loudspeaker driver in a 22.9×15.2×10.2 cm box with a passive radiator of the same size above the active driver, as shown in Fig. 3.1. The acoustic center was assumed to be at the center of the dust cap on the active driver. The directivity factor was measured according to a variant of ISO 3745, but with more measurement points than required to increase its accuracy and that of the sound power measurement.[2] Marquez recommended that the reference directivity source be one with a relatively smooth directivity pattern over frequency and angle, which means that for small errors in the reference angle, the error in directivity factor is likewise small.[7] The angles most used in this work were the principal

axis and those within 10 degrees of it, since these corresponded to the axes of highest output, resulting in a more favorable signal-to-noise ratio when measuring the room constant.

Fig 3.1. The reference directivity source in the anechoic chamber. The lower driver is an active loudspeaker, while the upper driver is a passive radiator.

3.3 The Reverberation Chamber

The venue primarily used for studying the limits of the two-point method when applied to large, extended sources is the smaller of two reverberation chambers on the Brigham Young University campus, pictured in Fig. 3.2. Its length, width, and height are approximately 5.69, 4.34, and 2.49 meters, respectively, corresponding to a room volume of 61 cubic meters. The floor is a concrete slab with an applied vinyl composition tile. The walls and ceiling are plastered and painted concrete and concrete masonry units. This room has an unoccupied reverberation time (RT60) of 6 s, calculated between (100 Hz to 10 kHz). Acrylic stationary diffusers are suspended from the ceiling to help increase the diffusivity of the field. The volume of this room

is similar to those of rooms used by Jensen and the author to conduct experiments on the large industrial noise sources.

An advantage of using a reverberation chamber for these measurements is that ISO 3741 sound power measurements (using squared pressure) can be carried out to have a benchmark to compare the two-point method against. Furthermore, the strong reverberant field typically yields favorable sound power results for most sources. Thus, measurements can be made in a best-case scenario in terms of the two-point method, compared to the standard results, then absorption can be incrementally added to the room to measure the effects as it approaches the mean absorption of the room containing the large industrial source and producing underestimated sound power results.

Fig 3.2. The small reverberation chamber on the BYU campus.

3.4 The Large Wooden Enclosure

In an effort to understand why a large, extended source would consistently cause the two-point method to underestimate sound power, the author sought to replicate such a source in a laboratory setting. It was impractical to obtain and relocate such a cumbersome source into the chamber, so instead, a large wooden enclosure was mocked up using 19 mm MDF with similar dimensions as the industrial source. Various loudspeakers and shakers were employed in and around the enclosure to simulate a distributed source. Its exterior dimensions were roughly $2.2 \times 1.2 \times 0.8$ m and it had an internal volume of approximately 2.1 m^3. Five removable panels could be replaced with different materials of varying transmission losses and radiation efficiencies. Foam gaskets along the borders of these panels allowed for airtight seals. These panels are discussed more in Chapter 4. The enclosure is photographed within the small reverberation chamber in Fig. 3.3.

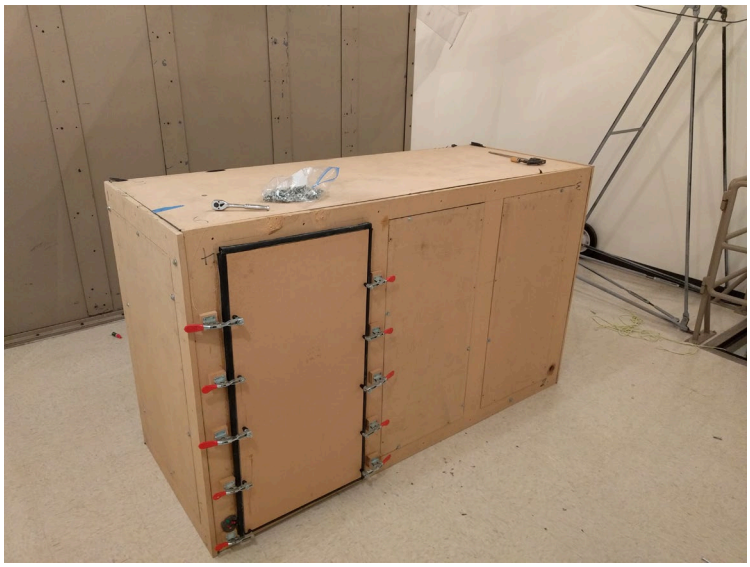

Fig 3.3. The large wooden enclosure assembled in the small reverberation chamber.

3.5 The Compact Source

A compact source was constructed to confirm the two-point method results of Marquez and Jensen, but to also allow for further research into the near-field behavior of compact sources and how the energy density eventually converges to far-field behavior. This source, shown in Fig. 3.4, was a 13 cm loudspeaker in a plywood box filled with polyester foam to enhance the compliance of the enclosed volume. It was powered using a Crown D-45 amplifier.

Fig 3.4. The compact source under measurement in the anechoic chamber.

3.6 The Line Array Source

A line array with 16 elements was designed to achieve a source with a non-spherically radiating near field, whose far-field directivity could be reasonably modeled and readily measured. This was built in order to evaluate the robustness of the direct term in the Hopkins-Stryker equation when applied to sources that violated the point-source assumption and had

dimensions large enough to guarantee that measurements were not in the direct far field. For a continuous line source, the radiation is subject to cylindrical spreading. In principle, the discrete line array can approximate this behavior at low frequencies. This array was built using 1/2" plywood and uses the same model of loudspeaker driver as the compact source, and each of the 16 drivers has a sealed volume behind it that is equal to that of the single-driver compact source. The drivers are connected in a series-parallel fashion so that the nominal impedance of the entire array measured approximately 8 Ω and all drivers are excited in phase with equal power. Its dimensions were 234 × 16.5 × 13 cm and can be seen pictured in Fig. 3.5.

Fig 3.5. The 16-element line array pictured in the large reverberation chamber.

3.7 ISO 3741

The sound power of the aforementioned sources was measured according to the ISO 3741 standard[1] to use as benchmarks for how well the two-point method performs under various test conditions. The standard requires at least 6 microphones, separated randomly throughout the

room as shown in Fig. 3.6. The microphones must be positioned a minimum of 1 meter from reflecting surfaces, 1.5 meters from the source, and $\lambda/2$ away from each other (1.7 meters at 100 Hz). The sound power calculation also requires that the total average absorption coefficient of the room be known, which is extracted from reverberation time measurements according to ISO 354, with six microphone positions and two source positions.[15]

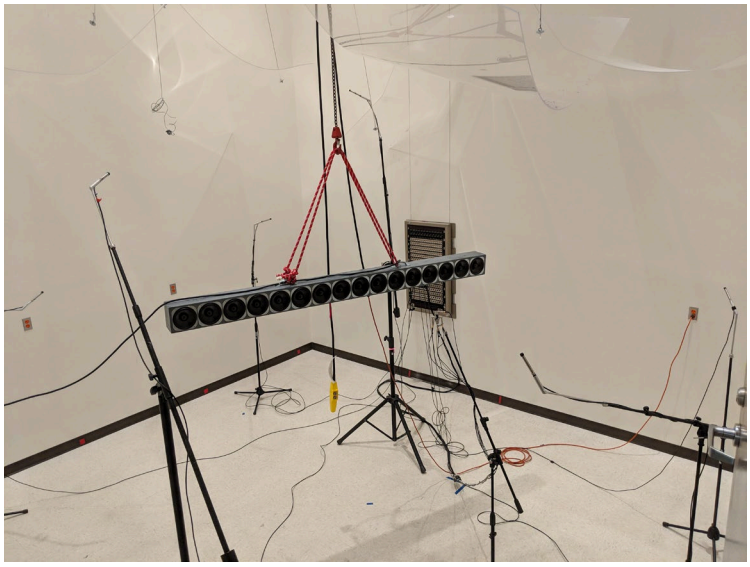

Fig 3.6. A setup in the large reverberation chamber for ISO 3741, including six microphones. The 16-element array is pictured in one of its measurement positions.

The compact source and the line array were both measured in the larger 210 m^3 reverberation chamber, whereas the various large wooden enclosure source configurations were measured in situ in the small reverberation chamber as pictured in Fig. 3.7. Since the working volume of the small reverberation chamber is relatively compact, some of the microphone and source position requirements were violated. Multiple measurements of compact sources in the large reverberation chamber, where specifications were properly met, were compared to

measurements with the violated setup in the small reverberation chamber. These comparisons showed that discrepancies between the two chamber setups were negligible for the purposes of this research.

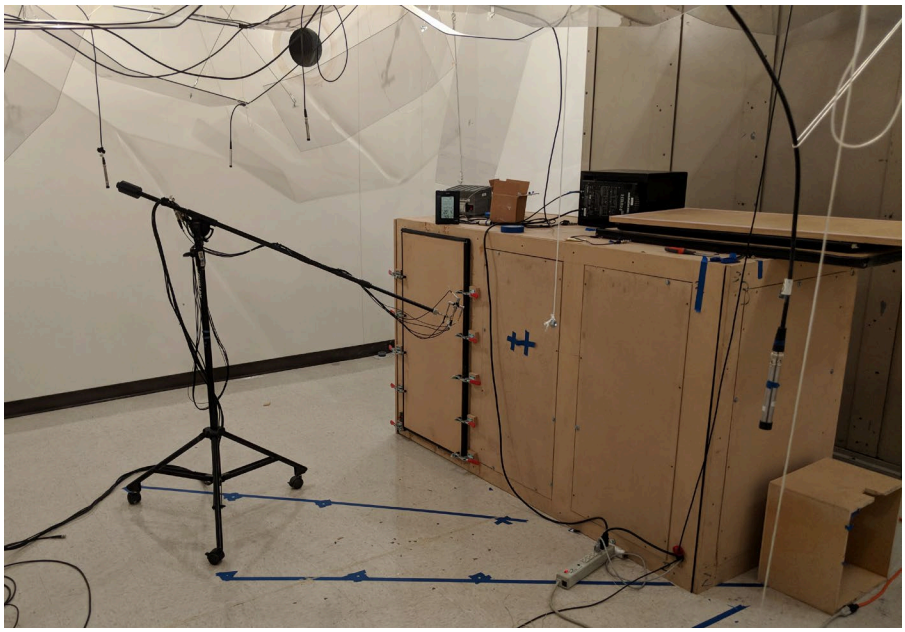

Fig 3.7. A setup in the small reverberation chamber for ISO 3741, including six microphones hanging from the diffusers. The large wooden enclosure is pictured in one of its measurement configurations. Loudspeakers are located on top of and inside the enclosure. The energy density probe is also pictured, since ISO 3741 measurements and two-point method measurements were taken simultaneously.

3.8 Directivity Measurements

At the time that it was determined to measure the directivity factor of the compact and line array sources, the high-resolution directivity measurement system had since been disassembled, so for simplicity and to maintain a timely progression of the research, it was decided to measure the directivity in only two planes. The horizontal (azimuthal) plane, and the vertical (polar) plane were measured by placing the source(s) on a remote-controlled turntable in

the anechoic chamber, and with a single microphone at 4.1 meters away, measuring the time-averaged squared pressure at five-degree increments over the 360 degree rotation. This setup is pictured in Fig. 3.8. This restricts the two-point method measurements to axes along these two planes (when using the measured directivity factor), but such a restriction is acceptable considering the scope of this study.

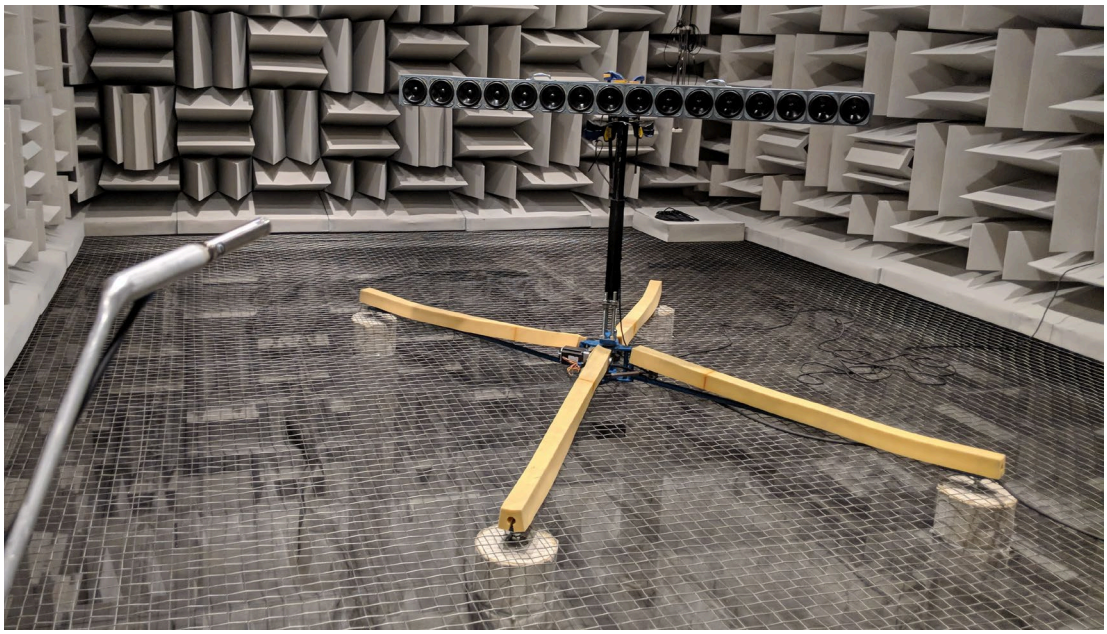

Fig 3.8. A setup in the anechoic chamber for measuring the directivity factor. The source is set up on a remote controllable turntable. Measurements are made at five-degree increments

As shown in Eq. (2.12), the directivity factor is defined as the ratio of the measured far-field intensity at some angle compared to the intensity of a monopole radiating with the same sound power. Once the mean square pressure measurements had been made along the 360 degrees, the numerator in Eq. (2.12) was calculated by applying the definition for time-averaged acoustic intensity,

$$\langle I(\theta_0)\rangle_t = \frac{\langle p^2\rangle_t}{\rho_0 c}. \tag{3.3}$$

The denominator was calculated by converting the measured sound power of the same source to intensity with the expression

$$\langle I_m\rangle_t = \frac{\langle \Pi\rangle_t}{4\pi r^2}, \tag{3.4}$$

where $\langle \Pi\rangle_t$ is the time-averaged sound power of the source as measured per ISO 3741 and r is the distance between the source and the microphone during directivity measurements.

Chapter 4

Experimental Results: Two-Point Method

The results of the two-point method experiments described in Chapter 3 are detailed in this chapter. The findings related to the two-point method applied to compact sources, distributed sources, and extended sources in a laboratory setting are shown and relevant discussion is included. Measurements of an industrial engine in a mechanical test cell are shown and analyzed. The behavior of sound power estimate results begins to diverge from expected values as the source becomes larger in size and as it radiates with a more complex sound field.

4.1 Compact Sources

The two-point method had previously been shown to properly estimate the sound power of sources that were relatively compact in nature to within 1 to 3 dB of ISO sound power measurements. Preliminary tests of the method conducted as part of this work confirmed these findings. One such test was of a Mackie brand studio loudspeaker measured using the two-point method. Results comparing the power estimate to the ISO 3741 measurement are shown in Fig. 4.1.

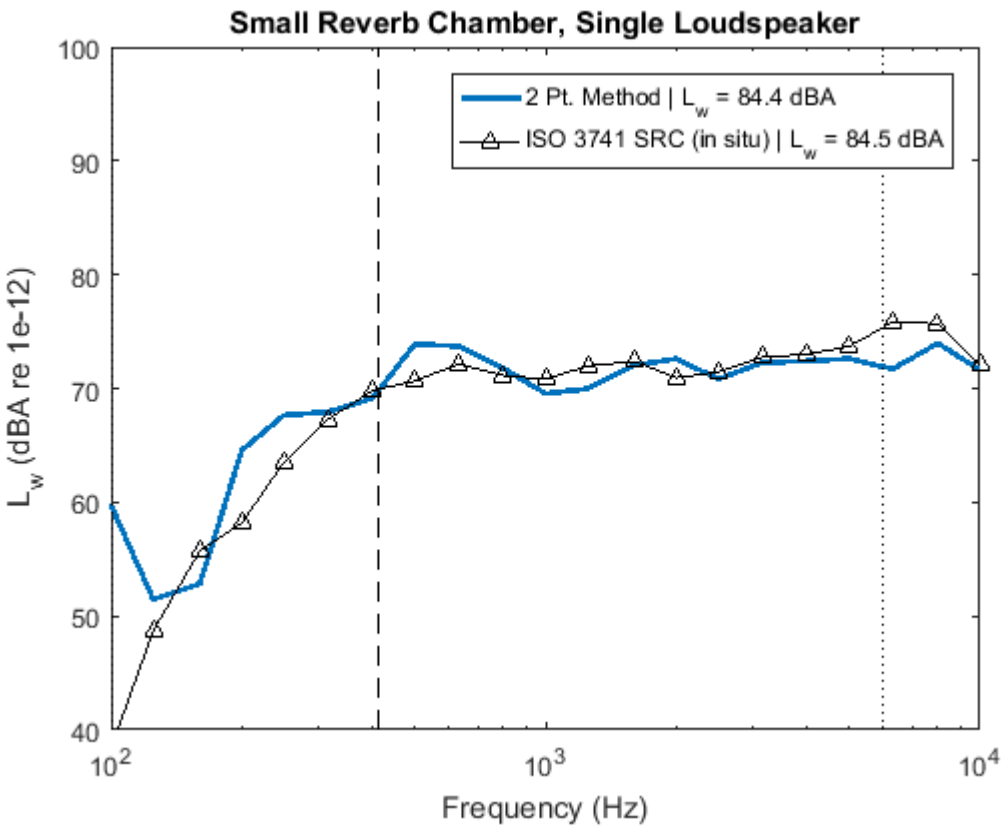

Fig 4.1. The sound power of a Mackie studio loudspeaker measured by the two-point method and per ISO 3741.

The vertical dashed line at roughly 330 Hz indicates the Schroeder frequency. Below this frequency, the diffuse field assumption inherent in the Hopkins-Stryker equation is violated due to strong room modes which dominate the behavior of the sound field. Therefore, results from frequencies below the Schroeder frequency are shown but not included in the calculation of overall sound power level values shown in the plot legend. Depending upon the particular sensor placement, results often agree somewhat with standard-measured values, but can diverge in other instances due to the strong room modes at low frequencies. While the upper frequency limit is dictated by the spatial Nyquist frequency (shown by the dotted line), results shown by Marquez and Jensen indicate that agreement between measured and expected values between 5,500 Hz

and 10,000 Hz was almost always maintained, so data for these frequencies are shown throughout this work.[7,8]

4.2 Distributed Compact Sources

One of the first experiments performed in search of circumstances that cause the two-point method to underestimate sound power was to place loudspeakers on and around the large wood enclosure to ensure that it was radiating from more than one specific acoustic center. This setup included a studio monitor on the ground adjacent to the opposite side of the enclosure from the probe, a studio monitor on top of the enclosure facing the probe locations, and a smaller speaker on the short edge of the enclosure. Each was powered with an orthogonal broadband excitation, so no two sources had the same signal output. Sound power measurements per ISO 3741 in this configuration in the small reverberation chamber are shown below in Fig. 4.2.

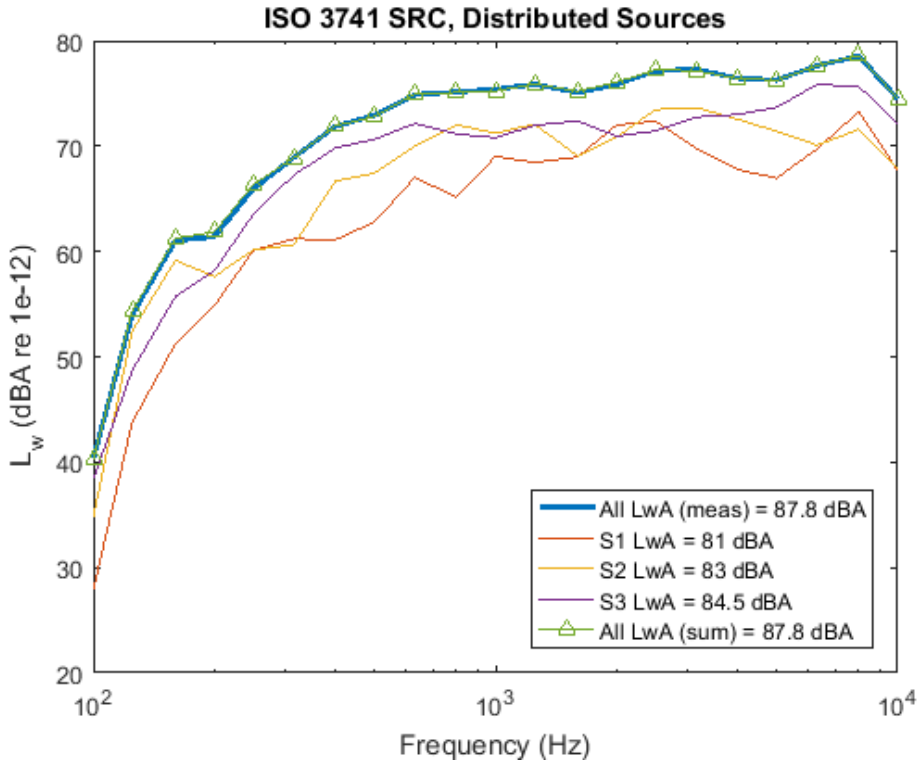

Fig 4.2. The sound power of three loudspeakers (S1, S2, and S3) adjacent to the enclosure measured per ISO 3741. The measured total and calculated total are shown.

To ensure that the sources were not coupling together, creating a total sound power that was different from the sum of their respective contributions, each of the sources was measured independently, then were measured together. The individual source measurements were then logarithmically summed and overlaid on the measured result. The summed and measured total power values agree for all frequencies, as shown. The two-point method was then used to measure the total sound power of the system. Results are shown below in Fig. 4.3 and compared to the ISO 3741 result.

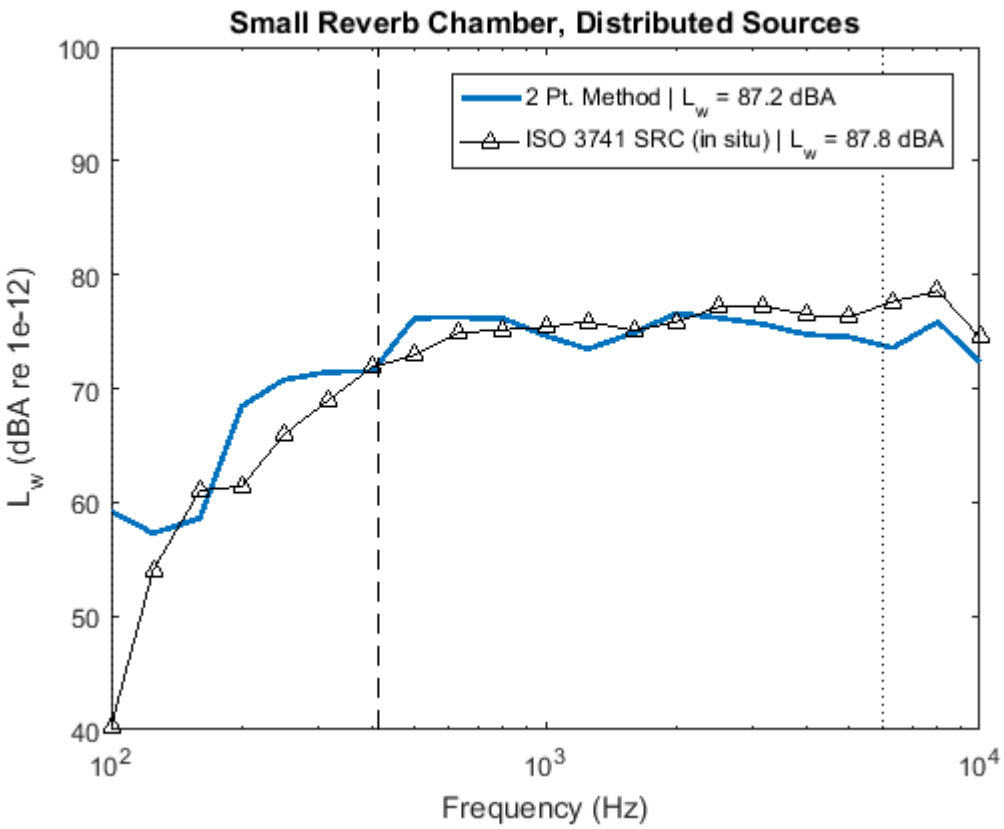

Fig 4.3. The combined sound power of three loudspeakers adjacent to the enclosure measured by the two-point method and per ISO 3741.

Although there were multiple acoustic origins present during this measurement, the two-point method appropriately handled the multiple sources and yielded an overall sound power that agrees well with the ISO 3741 result, with less than 1 dB difference in the overall result. Since the small reverberation chamber, even with a large wooden enclosure present, is predominantly reverberant, it is unsurprising that it works well in this configuration, since the reverberant term likely dominates the calculation of sound power. For this reason, acoustically absorptive urethane-based foam wedges were added to the small reverberation chamber until the RT60 (100 Hz to 10 kHz) was approximately 1.6 seconds, which required 30 wedges. The measurement was then repeated after measuring the room constant with the added absorption. The experimental

setup with the wedges is pictured in Fig. 4.4 and the results of this measurement are shown below in Fig. 4.5. The ISO 3741 microphones used for in-situ power measurements can be seen suspended from the diffusers.

Fig 4.4. The combined sound power of three loudspeakers adjacent to the enclosure measured by the two-point method and per ISO 3741.

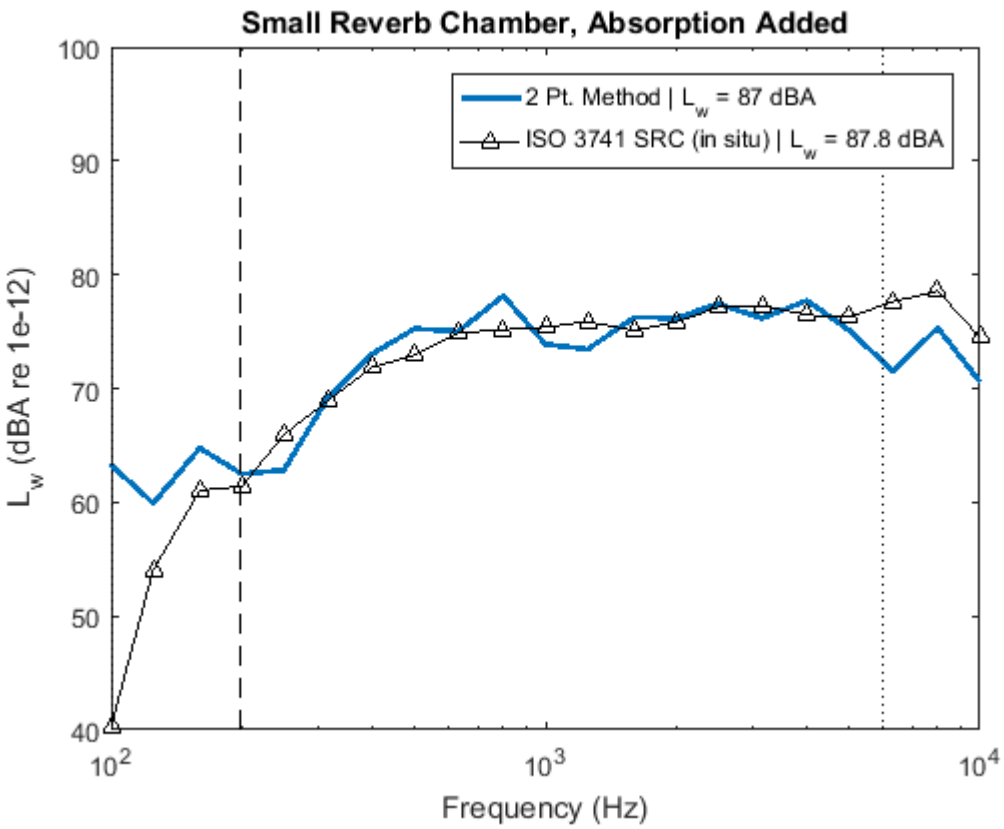

Fig 4.5. The combined sound power of three loudspeakers adjacent to the enclosure measured by the two-point method with absorptive wedges present compared to ISO 3741.

Since the two-point method again estimated the sound power to be near expected values, it suggests that the two-point method can estimate the sound power of multiple compact sources in semi-reverberant environments. While only these two results are shown, dozens of experiments in each of these configurations (with and without wedges with the three-source distribution) yielded similar results, showing robustness to sensor placement and the assumed acoustic center.

While this finding is significant, it did not provide any new information about what factors could be responsible for the underestimation observed when measuring large industrial engines. To continue the efforts to reproduce the underestimation in a laboratory setting, the large enclosure needed more complex radiation than the adjacent loudspeakers could provide.

4.3 Complex, Extended Sources

In this work, a distributed source refers to a source that is comprised of distributed compact sources about some geometry larger than the dimensions of any of the individual sources. An extended source refers to a source with large radiating surfaces, whose acoustic origin is less easily determined. The next experiment configuration included an 18” JBL powered subwoofer inserted into the MDF enclosure playing a high-amplitude square wave tone at 100 Hz, mimicking the piston-firing frequency of an engine. The low-frequency tone and its harmonics coupled to the volume of the enclosure and excited various modes and structural resonances of the enclosure walls, resulting in much more complex radiation that was still broadband in nature due to the structural excitation and square wave harmonics. The results from this experiment are shown below in Fig. 4.6. The same 30 absorptive wedges were present for this experiment. In order to measure the sound power per ISO 3741 for each experiment, the wedges are removed to return the small reverberation chamber to the reverberant conditions needed for that standard measurement. The sound power was then measured, then the wedges were returned to the chamber, and the two-point method measurement was performed.

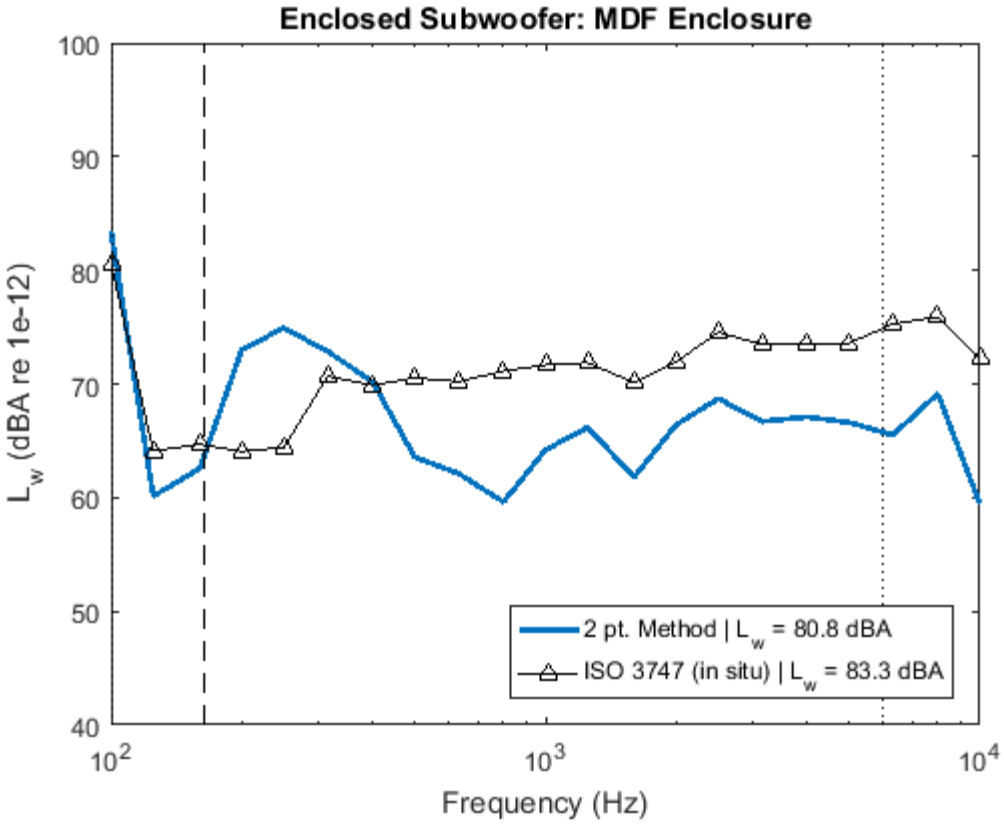

Fig 4.6. The sound power of the enclosure with a large subwoofer measured by the two-point method with absorptive wedges present compared to the ISO 3741 result.

This result represents the first evidence of underestimation reproduced in a laboratory setting. While the overall level falls short by 2.5 dB, the one-third-octave band results show more than a 10 dB disparity near 800 Hz. This is the most pronounced difference between the ISO 3741 and two-point method overall levels seen in laboratory experiments. The spectral shape shows that this underestimation is roughly uniform over frequency once above 500 Hz. This result was reproduced for various sensor positions, assumed acoustic origins, and measurement angles.

To further investigate the effect of this complex radiation on the two-point method sound power estimations, the enclosure was modified to force an even more extended source. Since the

large enclosure was repurposed from a previous experiment that tested the insertion loss of various panels, these panels were easily removed and replaced with three 1/4-inch Masonite panels and one 1/4-inch frosted acrylic panel. These had a much lower stiffness than the original 3/4-inch MDF and allow for additional structural excitation by the internal subwoofer, thus causing more extended radiation. In addition to the enclosed subwoofer, a large studio monitor was placed inside the enclosure and excited with white noise at maximum amplitude. Furthermore, mechanical shakers were affixed with epoxy to two of the Masonite panels and provided broadband excitation at the maximum rated power. This setup is pictured below in Fig. 4.7.

(a) (b) (c)

Fig 4.7. (a) The JBL subwoofer in the enclosure. (b) The enclosed studio monitor. (c) The thin Masonite and acrylic panels with shakers attached.

This system was then measured with the two-point method using two measurement points. The results from these measurements are shown in Fig. 4.8. The results again showed that the two-point method did not properly estimate the sound power of the system. However, the underestimation was not as pronounced as in the previous experiment, but it still falls several dB

below the ISO result across most frequencies, and the behavior is seen regardless of where the measurement line was chosen within the room.

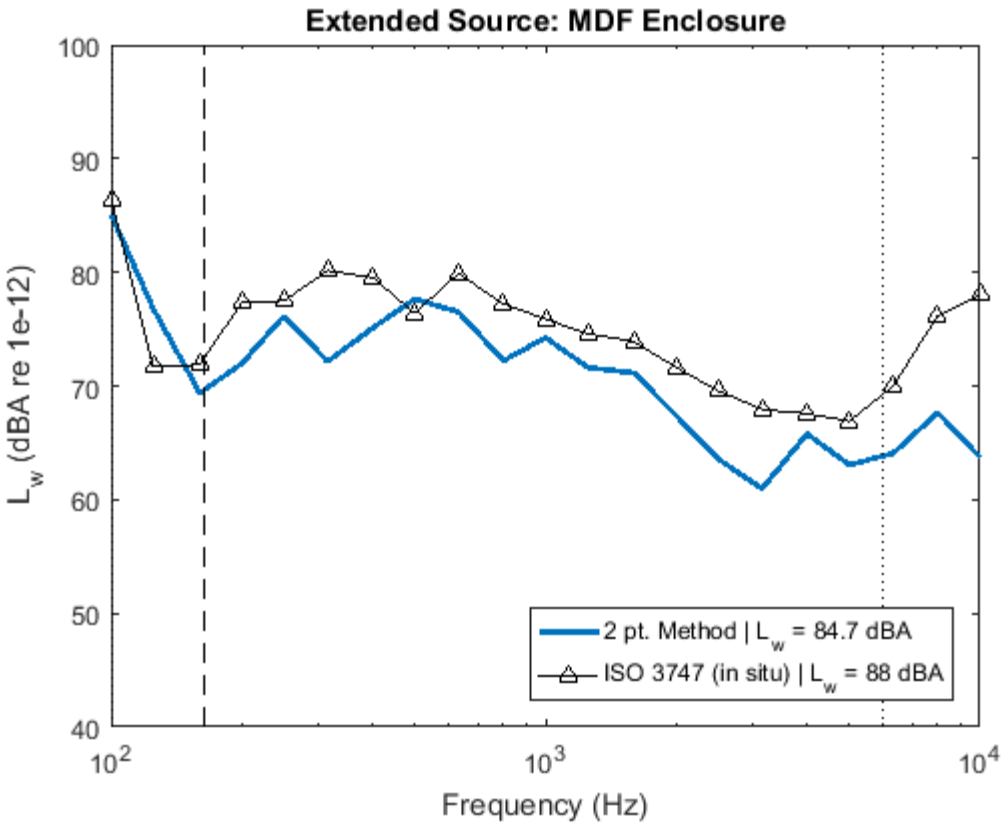

Fig 4.8. The sound power of the enclosure with thin panels, an enclosed subwoofer, and shakers rigidly attached to the enclosure walls measured by the two-point method with absorptive wedges present compared to the ISO 3741 result.

4.4 Engine Test Cell Measurements

Once laboratory measurements that showed the underestimation of sound power had been reproduced for complex, extended sources, additional data were taken on an industrial internal combustion engine at the research sponsor's mechanical test facilities. The conditions were similar to those of Jensen's tests, but with a different model engine and with different torque and

RPM configurations. The mechanical test cell measured approximately 5.5 × 7 × 4.5 m and had an RT60 (100 Hz to 10 kHz) of approximately 1.5 seconds. A 3D wireframe rendering of a typical mechanical test cell is shown in Fig. 4.9 below.

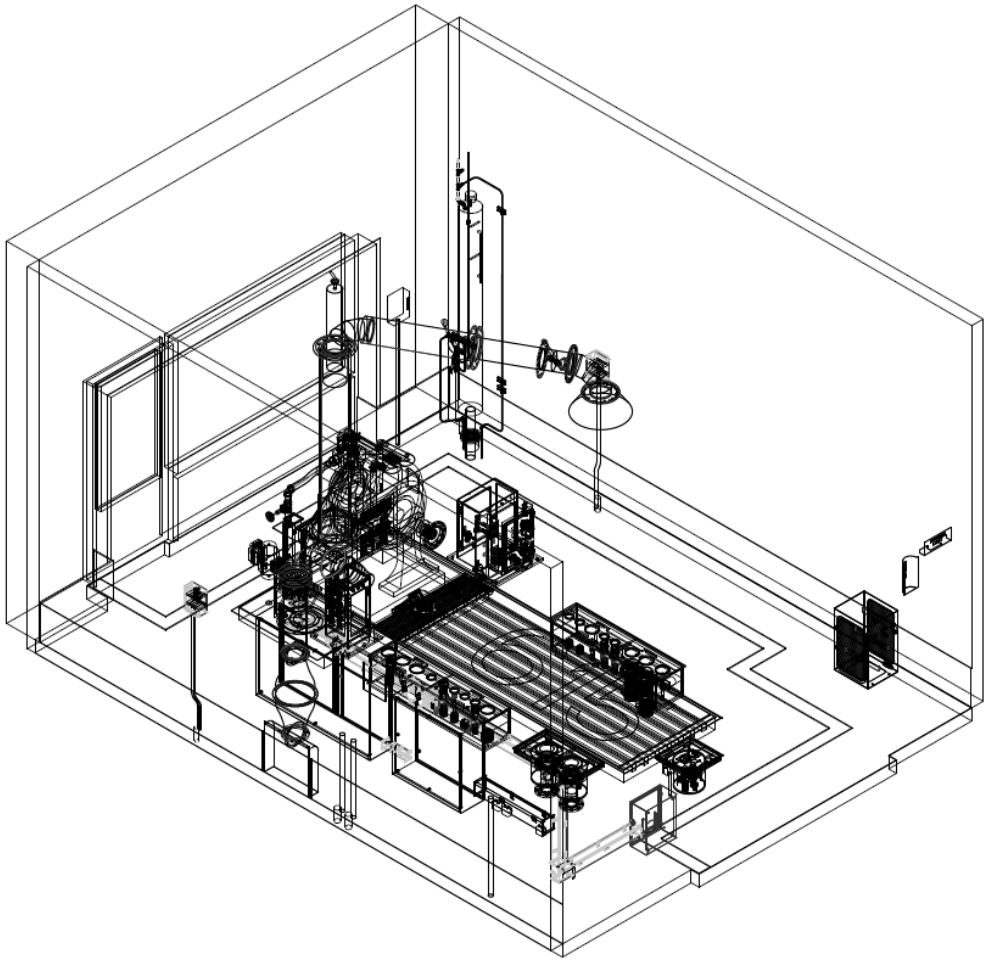

Fig 4.9. A wireframe rendering from the 3D model of the engine mechanical test cell where two-point method measurements were conducted at the sponsor's facilities.

4.4.1 Two-Point Method: Room Constant Measurements

To evaluate whether any of the underestimation could be a result of the acoustics of the mechanical test cell, the room was studied thoroughly before any engine measurements were

conducted. One of the recommendations made by Jensen for future work was to measure the room constant at various positions to obtain a better spatial average of the room. The room constant was measured using the reference directivity source (RDS) at multiple locations along 3 distinct axes in the test cell. A rendering of the probe measurement locations relative to the three RDS positions is shown in Fig. 4.10.

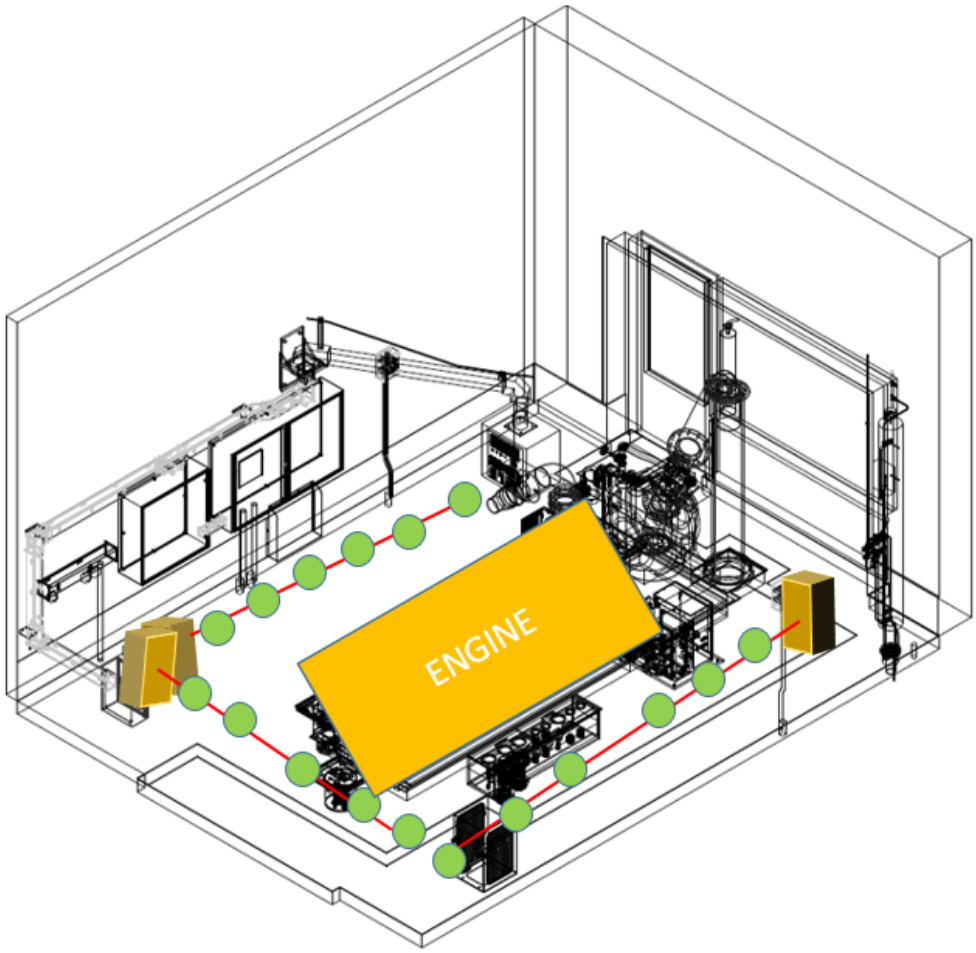

Fig 4.10. The measurement positions in relation to each of the three RDS positions. Each green dot corresponds to a probe sensor position in front of the RDS to measure the room constant.

The two-point method calculates the room constant using two GED measurements. Multiple combinations of measurement pairs were used along each of the three measurement axes to

understand the variation in the room constant measurement within the test cell. A total of 17 sensor positions were measured with the RDS to extract the room constant and to understand how the room constant varied depending on sensor position. While not within the scope of this work, the variation in the room constant in the test cells was studied. The room constant varies significantly depending on where in the room it is measured with the RDS, as shown in Fig. 4.11. In Jensen's work, it was found that the room constant often had an inconsistent shape across frequency, but this usually did not result in incorrect sound power results. The variation in room constant here though can influence the sound power result considerably.

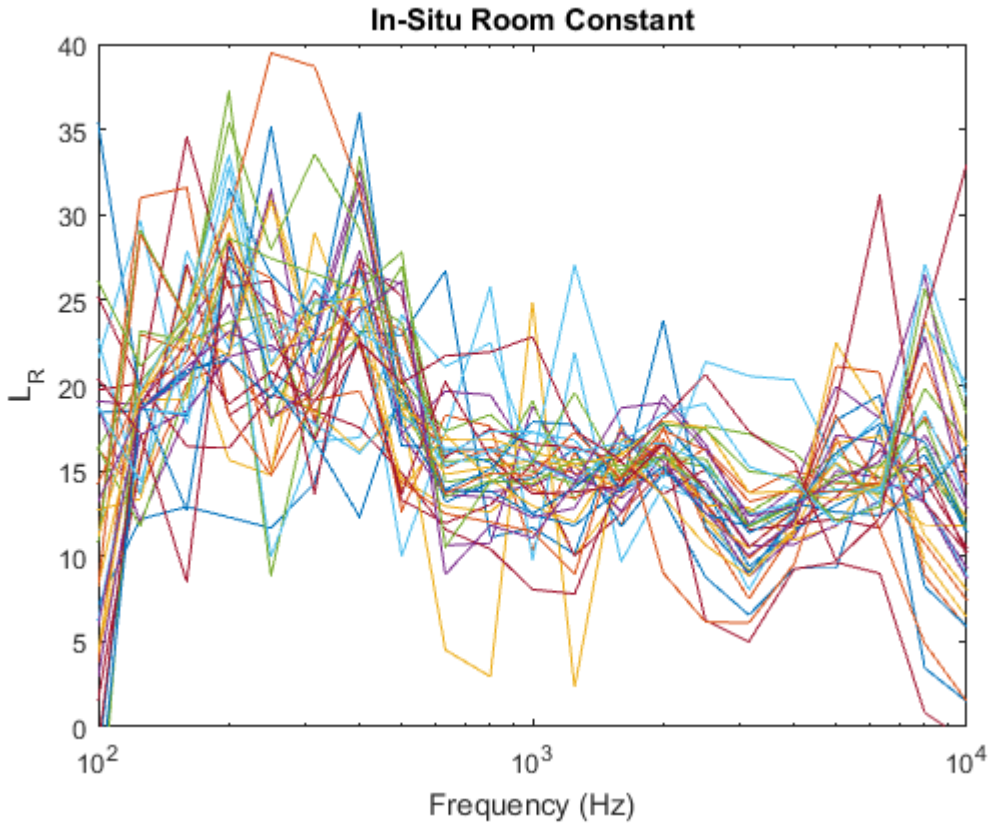

Fig 4.11. The multiple combinations of two-point method room constant measurement positions all shown on one plot on a logarithmic scale. There is significant variation between different measurement pairs.

In order to reduce the multiple measurements to a single useful room constant, these were averaged together, then smoothed with a moving average across frequency to reduce the result to one similar to the estimated room constant derived from the RT60. The mean room constant is plotted with the RT60-derived room constant in Fig. 4.12.

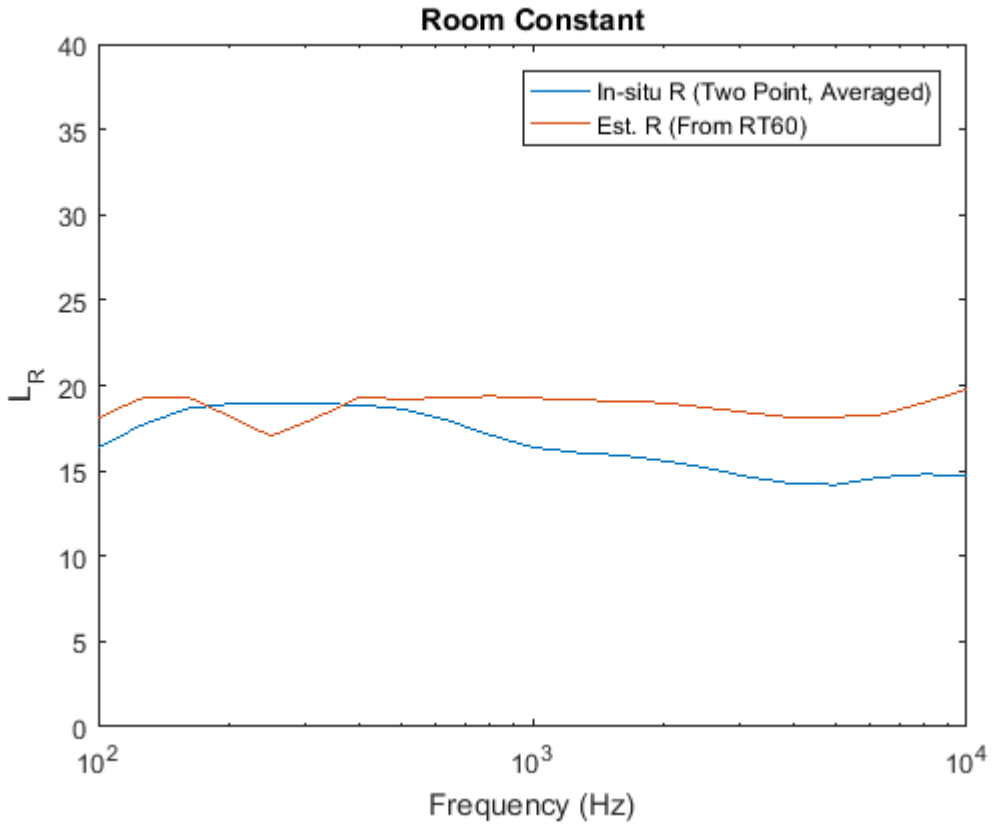

Fig 4.12. The room constant shown on a logarithmic scale after having been averaged and smoothed (blue) compared to the estimated room constant (red) derived from the RT60.

4.4.2 Dodecahedron Measurements

One experiment of interest was to measure the sound power of a compact source within the mechanical test cell with the engine present but powered off. This experiment would help confirm whether the room acoustics were a factor in the underestimation of engine sound power,

because if the sound power of the compact source was successfully measured in the test cell, it would suggest that the discrepancies are due to the source, and not the environment. The compact source that was selected for this experiment was the dodecahedron VVS, or volume velocity source, previously provided by the author to the research sponsor as part of an adjacent project. It consists of twelve loudspeakers arranged in a dodecahedron frame with a spherical outer diameter. The quasi-omnidirectional nature of this source with its high output and compact footprint make it an ideal candidate for this experiment. Additionally, sound power data per ISO 3741 were readily available for this source. A photograph of the VVS in the test cell is shown below in Fig. 4.13.

Fig 4.13. The VVS mounted on a tripod during measurement of the sound power per the two-point method. The tripod-mounted energy density probe is also shown.

The two-point method properly estimated the sound power of the VVS within the test cell, with the engine present but powered off. This confirms that the anomalies seen in the engine data are due to the source, not the acoustics of the room, since a compact source was measured correctly by the two-point method in the mechanical test cell. This result is shown in Fig. 4.14.

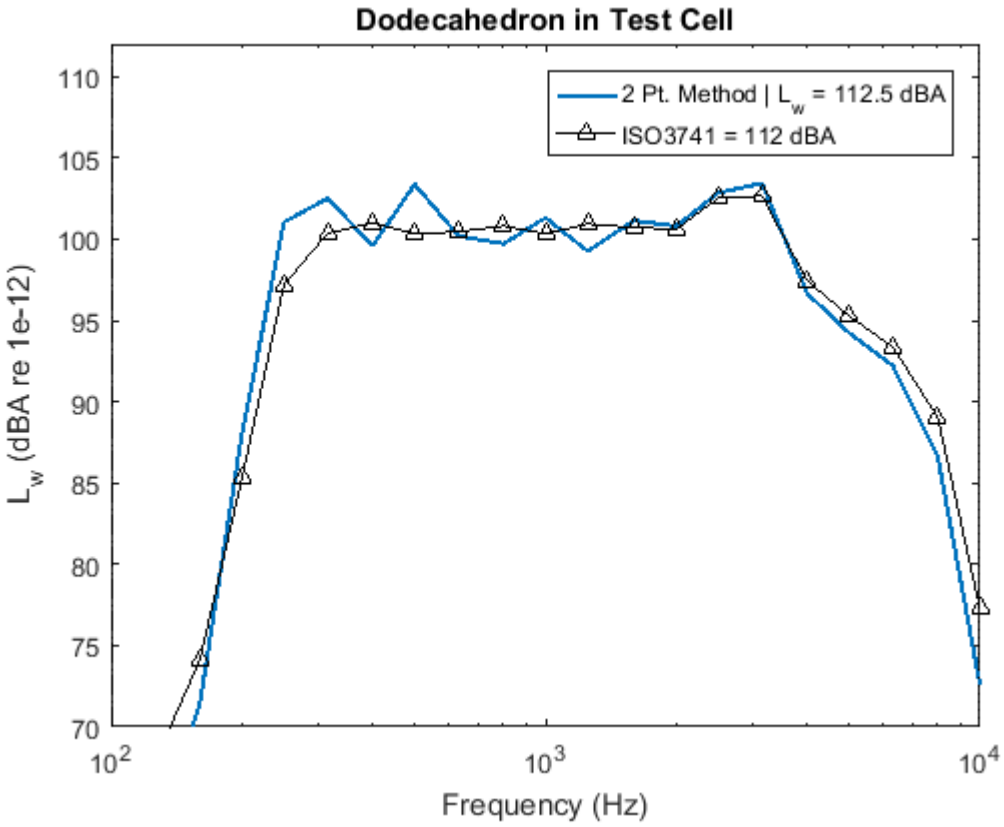

Fig 4.14. The sound power of the VVS measured in the test cell with the engine present but powered off. The ISO 3741 result for the source is also shown.

4.4.3 Engine Measurements: ISO 3747

In order to make a useful assessment of the two-point method, the sound power of the engine was measured according to ISO 3747:2010 which is referred to as the "comparison method."[15] This survey-grade standard measurement procedure employs the reference sound

power method. A Brüel and Kjær type 4224 sound power reference source was placed around the engine at six distinct locations and the sound pressure levels were measured by twelve free-field microphones scattered randomly about the room. From these measurements, the in situ room constant was obtained in a manner similar to the procedure for the two-point method. This setup is pictured in Fig. 4.15.

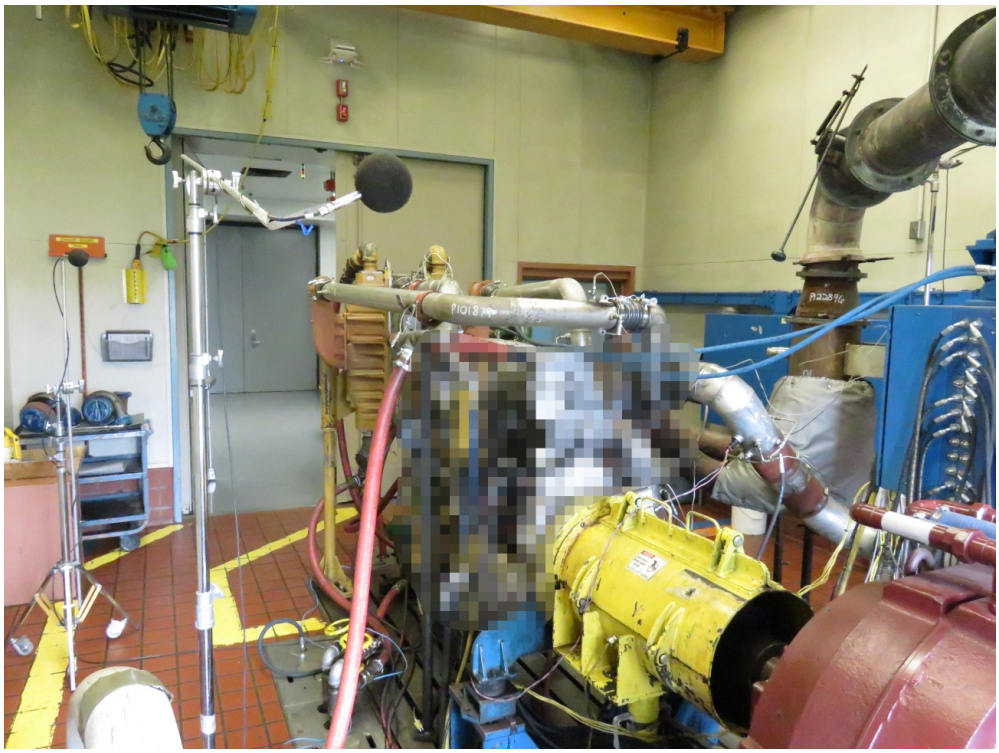

Fig 4.15. Several of the ISO 3747 microphones (with windscreens) pictured around the engine. These pressure measurements are used to calculate the sound power of the engine by comparing to the pressure of a source with known sound power.

The engine was then powered on and several sound power measurements were made at various engine speeds and loads using the pressure from the microphones. The sponsor, who conducted these tests, has used this measurement standard in tandem with ISO 3741 and ISO 3745 tests and is familiar with best practices that yield ISO 3747 results that are comparable to

the precision standards. Some of these practices include taking multiple pressure averages with the reference sound power source in various places around the room, ensuring that microphones are in line-of-sight with the engine and the reference source, and removing any outliers in reference source pressure measurements due to proximity of the reference source to the microphone(s). With these measures in place, the ISO 3747 results are given with confidence that the survey-grade standard is properly estimating the power.

In order to protect sensitive information relating to the products of the sponsor, once results had been processed and discussed internally, the sound power data were recomputed with various arbitrary references. These are similar to the typical sound power level reference of 1 picowatt, but vary depending on the engine condition to obfuscate sensitive information. Because each comparison is made to the same arbitrary reference power, meaningful direct comparisons between the two-point method and ISO 3747 levels are maintained. Different engine conditions are given different reference values, however. All engine data contained in this thesis is subject to this modification.

4.4.4 Engine Measurements: Two-Point Method

The engine was measured at various points along three main axes, shown by the red lines and green circles in Fig. 4.16. One axis was chosen to be diagonal off the corner into the most open portion of the room but remained at the same height as the engine. This is referred to as “Diagonal 1” and is shown in the bottom left corner of the room in Fig. 4.16. Another axis, “Diagonal 2,” extends from the opposite corner of the engine and extends out-of-plane up into the corner of the room near the ceiling, shown in the top right of the diagram. A final axis was chosen to be perpendicular to the edge of the engine between the engine and the wall, referred to

as “Perpendicular 1.” The two diagonal axes contain four measurements each, two located near the engine, and two located beyond the roughly estimated critical distance of 1.5 meters. The perpendicular case only had space for two measurement positions between the engine and the wall. Table 4.1 shows each of the distances from the geometric center of the engine to the sensor location.

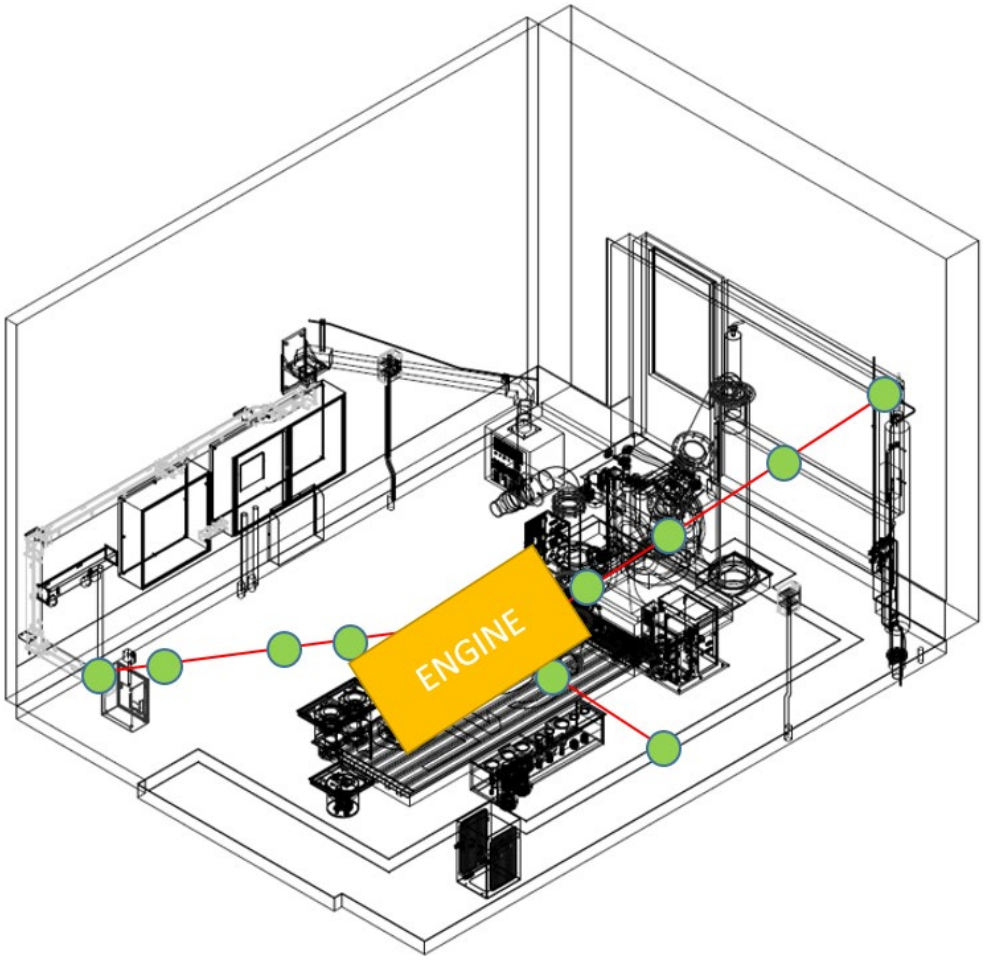

Fig 4.16. Diagram showing the approximate locations of the sensor measurement positions. The left axis is “Diagonal 1,” the one in the top right is “Diagonal 2” and the one going toward the bottom right is “Perpendicular 1.”

Table 4.1. The measurement distances from the geometric center of the engine to the sensor locations.

Diagonal 1 (m)	Diagonal 2 (m)	Perpendicular 1 (m)
1.01	0.937	0.978
1.59	1.47	2.336
2.73	2.89	
3.4	3.52	

The engine sound power results measured by the two-point method (using the mean room constant) for one specific engine configuration, referred to as “Engine Condition A” are shown in Fig. 4.17. Along each measurement axis, significant underestimation ranging from approximately 5 to 8 dB is observed.

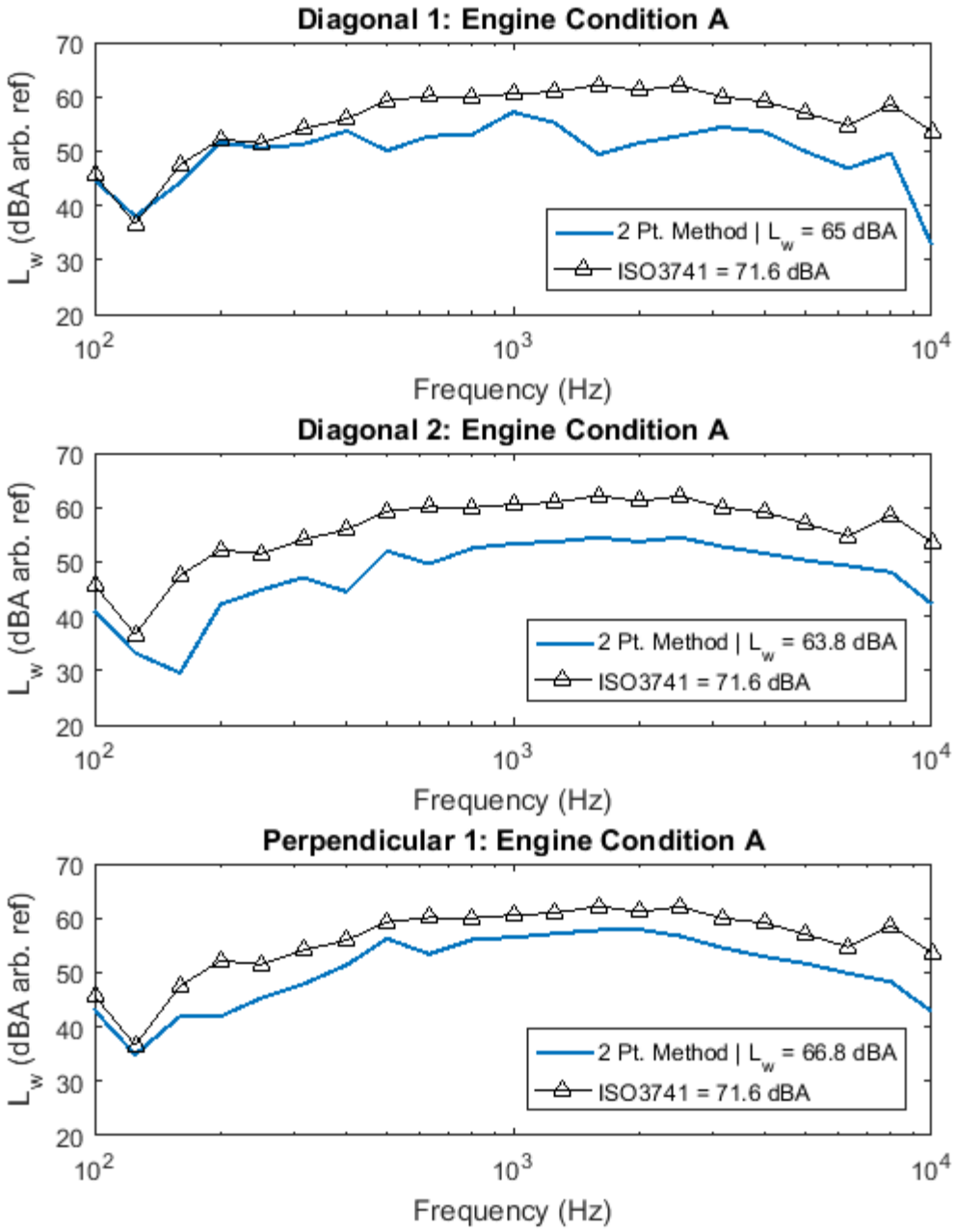

Fig 4.17. The sound power of the engine operating under condition A as measured by the two-point method along three different axes.

The torque and RPM were then altered and named “Engine Condition B.” The results in this configuration show similar underestimation ranging from 3 to 7 dB, as shown in Fig. 4.18.

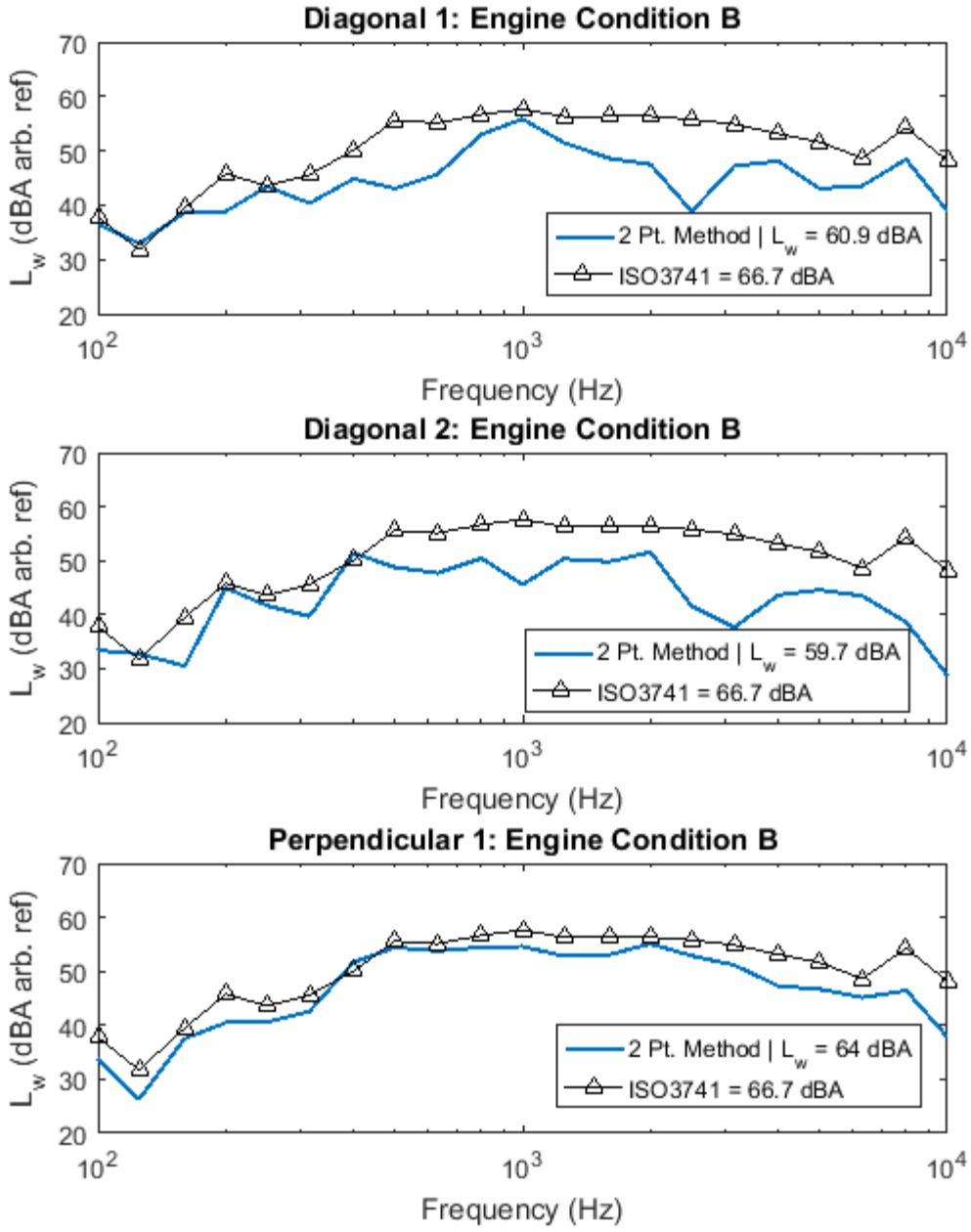

Fig 4.18. The sound power of the engine operating under condition B as measured by the two-point method along three different axes.

Since the room constant, GED measurements, and r values had been thoroughly investigated, the only remaining variable of interest in the Hopkins-Stryker equation was the directivity factor γ. The directivity factor of the DUT is not typically of interest since the power is what is often of importance. However, in the script calculation, the system of equations is broken into intermediary calculations that include solving for the directivity factor of the DUT, that are then fed into the final calculation that returns the sound power. When the directivity factor for these engine measurements was observed, the results were unexpected. Figure 4.19 shows a sampling of three directivity factors that are indicative of the behavior of each measurement that showed significant underestimation.

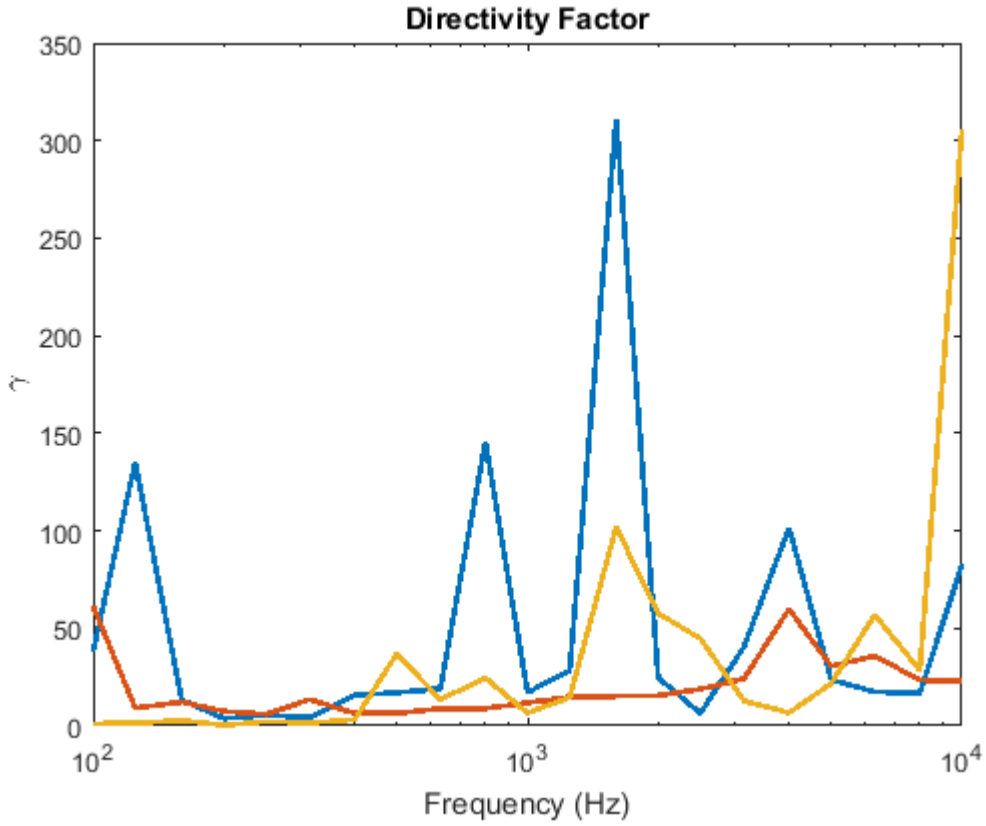

Fig 4.19. The derived directivity factor of the engine as calculated by the two-point method.

The directivity factor, as detailed in Chapter 2, is expected to be 1 for an omnidirectional source. For a simple source radiating in a trihedral corner, a directivity factor of 8 would be expected. Highly directional horns can achieve directivity factors of 40 and above in practice.[16] To see adjacent one-third-octave bands jump from 20 to 300 is simply nonphysical. While an engine likely has a very complex directivity, it is expected that low frequencies will be near 1, with a gradual, albeit uneven, increase as frequency increases. This result prompted the separate investigation into the directivity factor itself described in Chapter 3 by building an array and measuring the directivity factor to then use in two-point method calculations to gain additional insight into the direct (and reverberant) terms in the Hopkins-Stryker equation.

4.5 Anechoic Chamber Measurements: The Direct Term

One of the most apparent assumptions in the direct term of the Hopkins-Stryker equation is that of spherical spreading. The $1/4\pi r^2$ term describes the spherical propagation of the acoustic intensity between the source and the measurement position. The propagation of a continuous line array, however, would be expressed as $1/2\pi r$. The discrete line array built for this experiment should have some behavior between the two. The GED was measured in front of the line array along a 4 meter traverse. It was then repeated at a 45-degree angle. The results on a log scale are shown in Fig. 4.20. Superimposed on the plots are the slopes for $1/r^2$ behavior and for the $1/r$ cases. It can be seen that on axis near the array, it behaves more similarly to a cylindrical wave with $1/r$ spreading, then converges to a decay slope that is between the two cases. The 45-degree case follows the $1/r$ slope for about a meter, then falls off quickly and converges to the

$1/r^2$ slope. This confirms that the line array has a radiation that is more complex than can be described by simple spherical spreading.

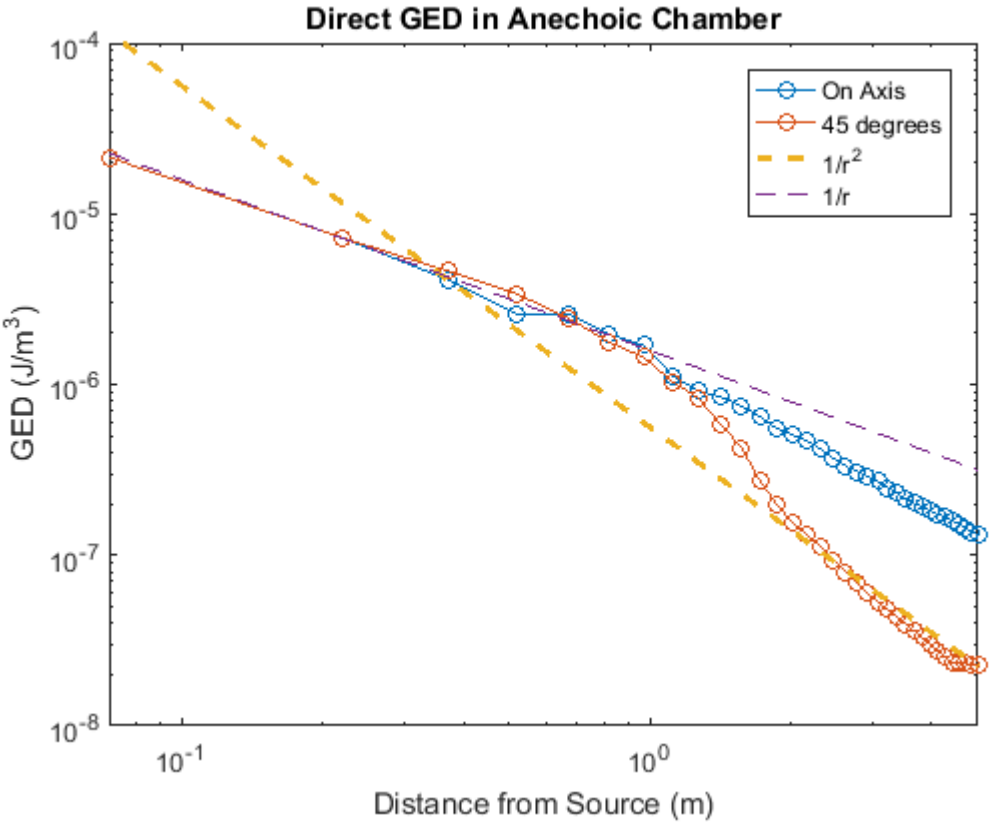

Fig 4.20. The GED as a function of distance for the line array measured in the anechoic chamber.

To compare to a more conventional source, the measurement was repeated for the single array element in a box. The results for this measurement are shown in Fig. 4.21. As expected, the compact source radiates according to the $1/r^2$ decay slope. The 45-degree case sees reduced GED compared to the on-axis case due to the directional nature of a front-facing loudspeaker, but both see a similar slope.

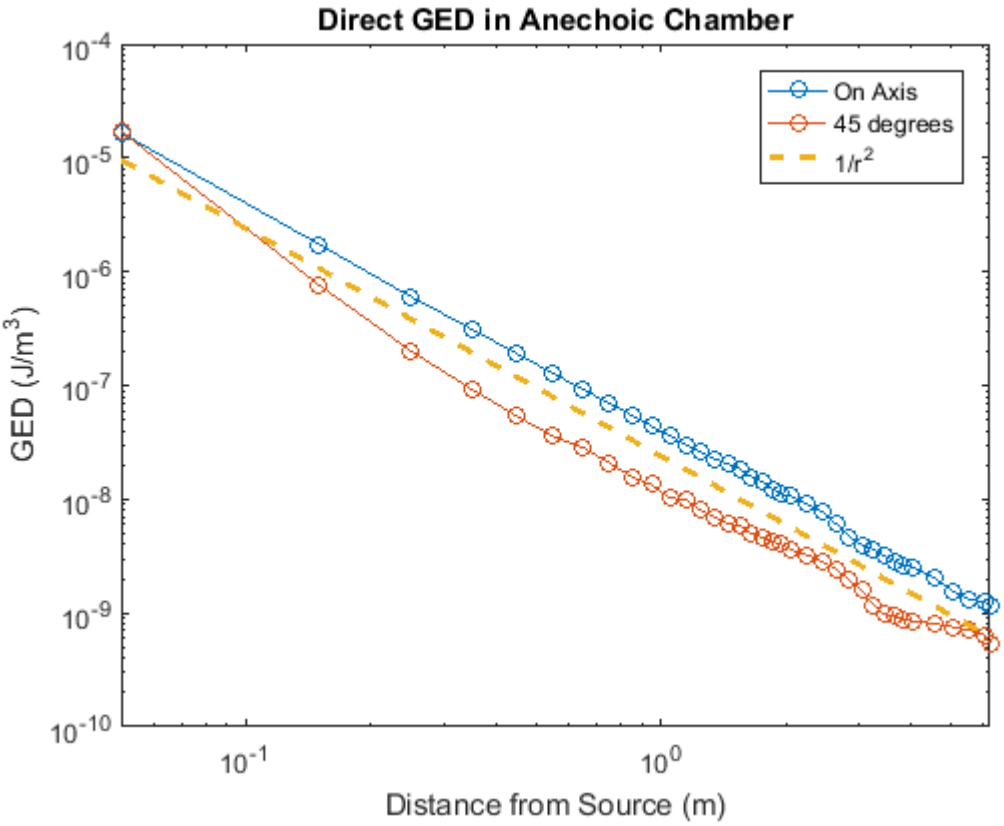

Fig 4.21. The GED as a function of distance for the compact source measured in the anechoic chamber.

Understanding the limitations of the spherical spreading model is only half the picture of the direct term in the Hopkins-Stryker equation. The remainder of the term contains the directivity factor. This was measured in the anechoic chamber for both the array and the compact source. The directivity index, which is a representation of the directivity factor but normalized to the result of maximum response (typically the principal axis) is shown in Figure 4.22 for a few frequencies with both the horizontal (the array oriented horizontally) and vertical axes.

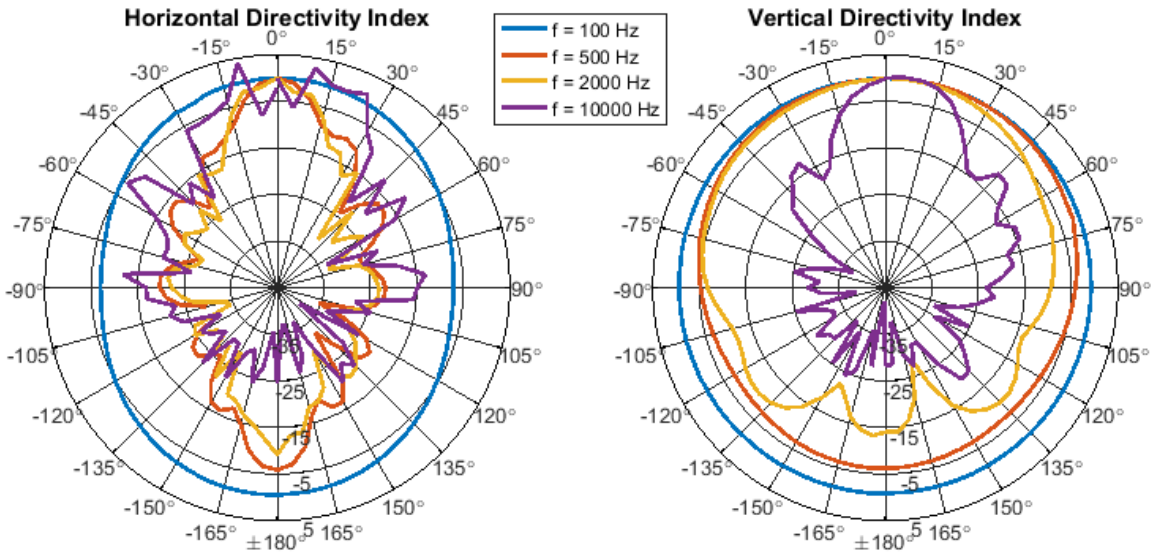

Fig 4.22. The directivity index at various frequencies of the line array in the horizontal and vertical directions.

The horizontal directivity factor of the array is shown on a cartesian plot in Fig. 4.23.

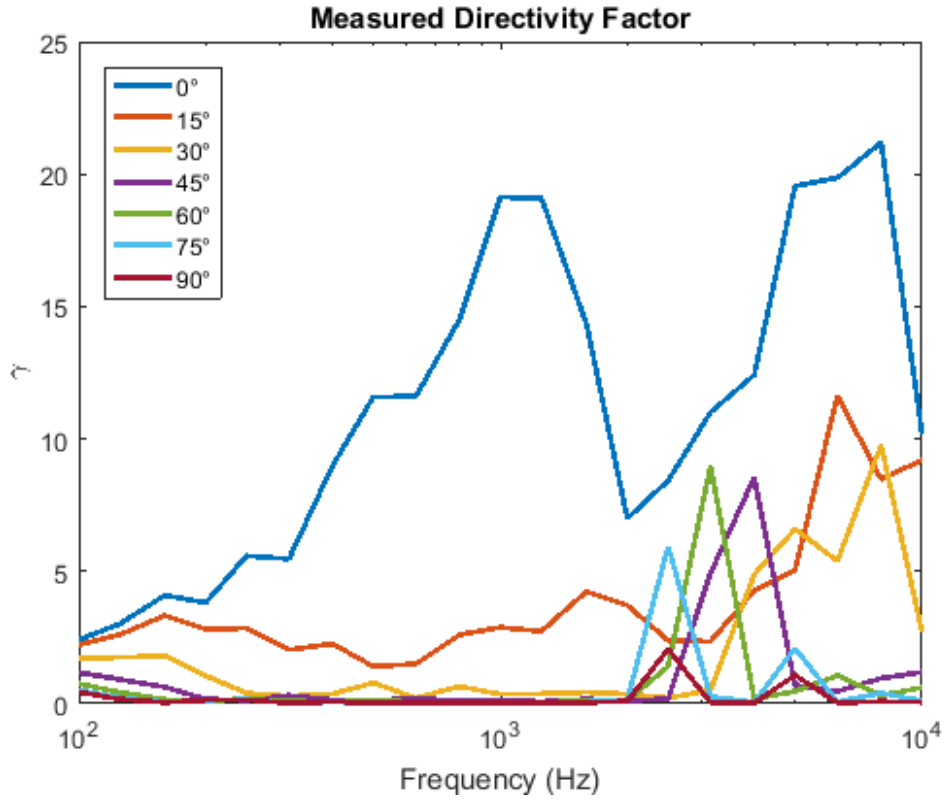

Fig 4.23. The directivity factor at various angles of the line array in the horizontal direction.

Since the primary axis falls between two loudspeaker drivers on the array, the strange behavior seen on axis is likely due to angular error during measurement, mutual coupling and cross-path cancellation. At other angles, it behaves expectedly, where it radiates very little (nulls) except for large peaks (lobes) that vary spatially and in frequency.

The directivity factor for a single compact source is shown in Fig. 4.24 and shows much more expected behavior with low frequencies near 1 and gradually rising to higher values at higher frequencies primarily on and around the principal axis.

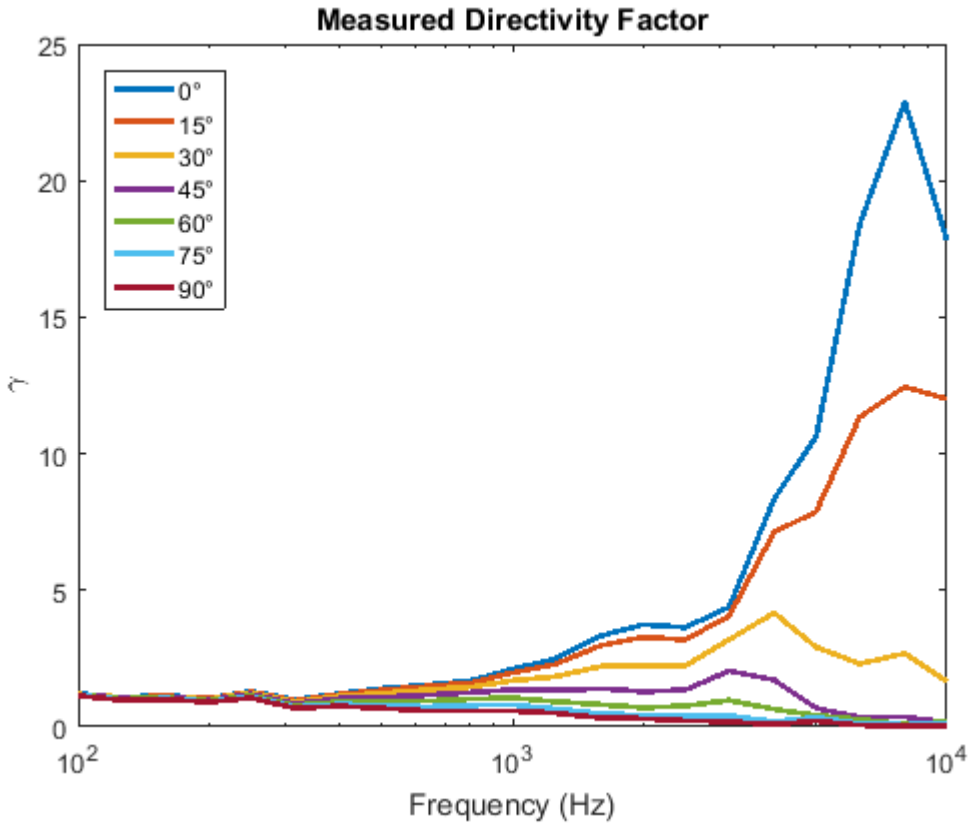

Fig 4.24. The directivity index at various frequencies of the compact source in the horizontal and vertical directions (symmetry assumed).

Since the directivity factors are known, they can be used in the two-point formulation to replace one of the degrees of freedom in the sound power calculation with measured data.

In the anechoic chamber, the two-point method was used to measure the sound power of the array on its principal axis. Since the room constant is essentially infinite in a free field, only the direct term was used in the calculation. The two measurement positions in this case were roughly 0.3 m and 1.3 m and the measured directivity factor was used in the calculation. This result is shown in Fig. 4.25.

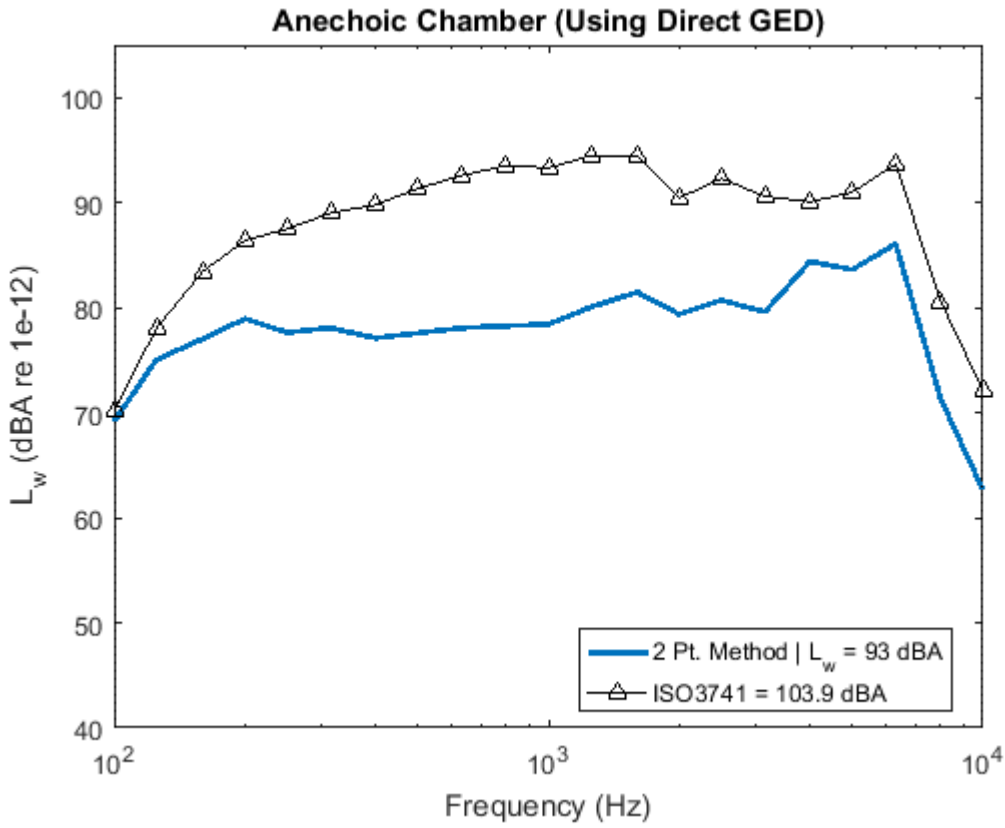

Fig 4.25. The sound power of the array measured by the two-point method (direct term only) in the anechoic chamber. One measurement position was in the near field, and the other was approaching the far field.

This result is especially interesting because even with the measured (far field) directivity factor, the two-point method once again underestimates the sound power of this extended source.

However, when measurement points are selected in what is considered to be the far field, the result is very different, as shown in Fig. 4.26.

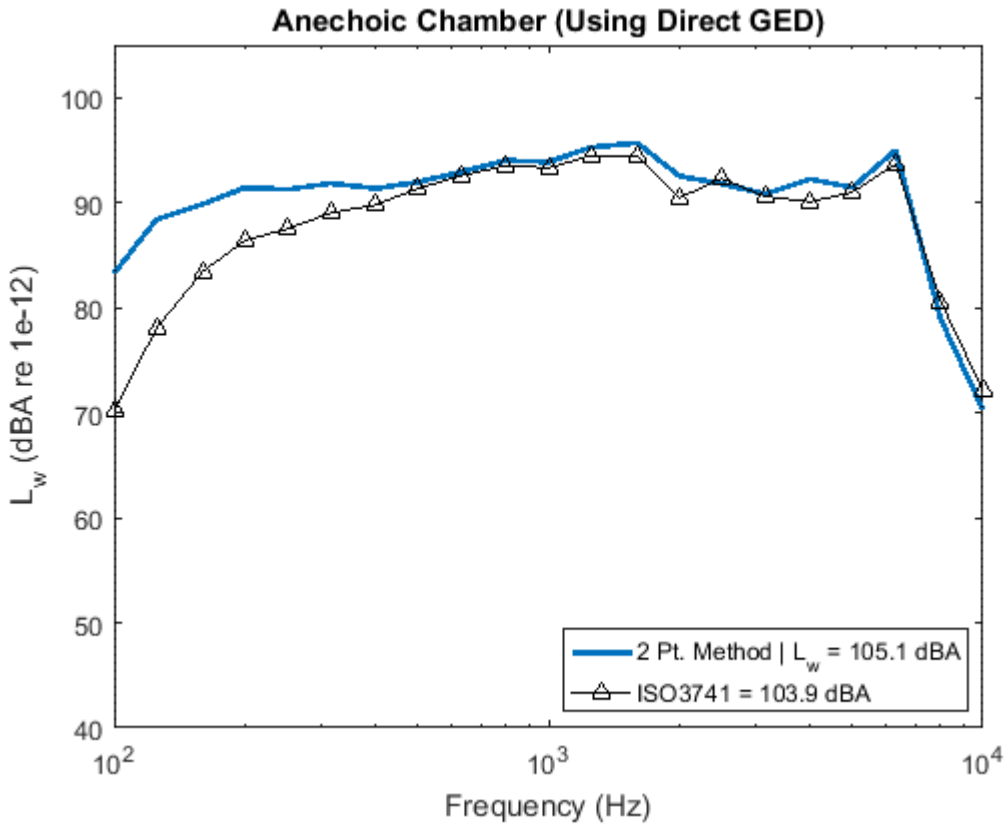

Fig 4.26. The sound power of the array measured by the two-point method (direct term only) in the anechoic chamber. One measurement position is in the far field.

In this case, above 500 Hz, the sound power matches the ISO sound power result almost exactly. This suggests that the underestimation may be more influenced by the direct term formulation in its entirety, rather than just the directivity factor. Considering the findings shown in Fig 4.20, if the field is sampled where radiation is more consistent with cylindrical spreading, and then sampled in the far field where it is more closely resembling spherical spreading, it is unsurprising that this introduces errors.

4.6 Reverberation Chamber Measurements: The Reverberant Term

Although the room constant is relatively well understood and the reverberant term is rather simple with only two terms, in the reverberation chamber it is possible to experimentally recreate the simulated plot in Fig. 2.1 and determine the critical distance to compare it with the one calculated in the measurements according to Eq. (2.9). Figure 4.27 shows this result graphically. The direct energy (circle lines) falls off and eventually levels out as it reaches the steady-state reverberant energy of the room (black dash line). For the on-axis case, the critical distance is approximately 1.8 meters (blue vertical dash line). For the 45 degree case, it shortened somewhat out to 1.45 m (red vertical dash line).

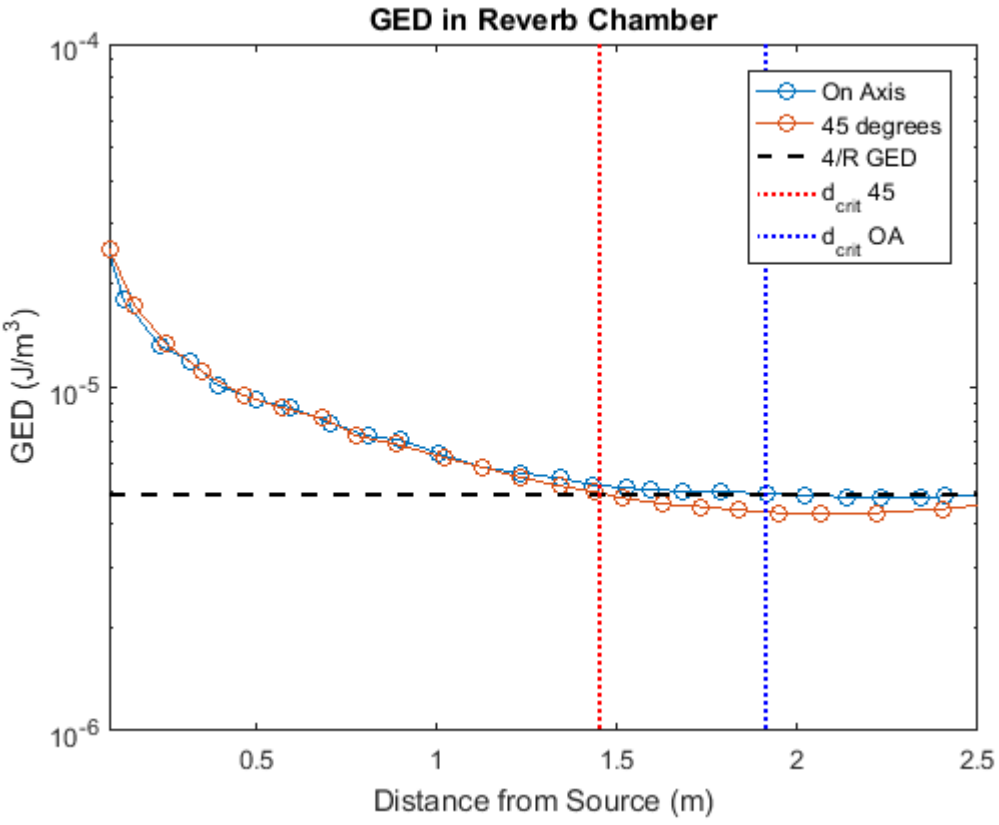

Fig 4.27. The GED as a function of distance for the line array in the reverberation chamber.

The critical distance calculated for this case according to Eq. (2.9) was 2.3 m. This discrepancy suggests that there is an issue with how the Hopkins-Stryker equation describes the energy density when applied to large, extended sources. Even when the directivity factor, room constant, and measurement distances are well known, measured and calculated values still do not agree for this source. The critical distance, by definition, also depends on the direct and reverberant energies being equal and this work has determined that the behavior of the direct field for extended sources is very different from that of compact sources, so this discrepancy is somewhat expected.

4.7 Results Discussion

As has been covered in this chapter, the two-point method is unable to accurately estimate the sound power of large, extended sources when measurement positions are included that are in the near field of the source. Even with the measured directivity factor, the method fails when measured close to the source. This is likely due to the radially dependent directivity factor. It was measured in the far field, but when applied to measurements in the near field, the true directivity factor could be very different from that which is being used. Furthermore, the direct term, even when adjusted to more closely resemble other source behaviors, does not allow for straightforward near-field measurements with acceptable results.

While the recommendation of Marquez to place one measurement position within the critical distance and one beyond the critical distance works well for compact sources, any inclusion of near-field measurement points distorts the measurement significantly for large, extended sources. In a laboratory environment, the underestimation was reproduced for many

near-field measurement positions, only to have it converge to a result much closer to the ISO standard results once several meters away from the source. These findings led to the development of a more simplified deployment of the two-point method. This is discussed in detail in Chapter 5.

Chapter 5

The Simplified GED Method

The results of the two-point method showed that it is difficult to consistently obtain meaningful sound power data of large, extended sources. The difficulties surrounding the direct term and the violations to the assumptions in the Hopkins-Stryker equation in the measurement of engines in mechanical test cells are unable to be resolved to allow the two-point method to be a feasible solution for measuring the sound power in these test cells. However, in an attempt to still provide an efficient and robust measurement procedure to the sponsor, certain simplifications were explored to see if it was possible to obtain meaningful sound power data from GED measurements, even if only to survey-grade accuracy.

5.1 Simplifications to the Two-Point Method

As discussed in Chapter 4, the underestimation of sound power by the two-point method when applied to large industrial engines is caused in part by erratic behavior in the room constant, the incorrectly derived directivity factor of the engine, and the overall effect of the

direct term in the sound power formulation. In particular, the erratic spectral shape of both the in situ room constant and directivity factor heavily influenced the final result. In order to mitigate the effect of these, simplifications were introduced to the method.

The first simplification was to eliminate the need for the two-point method to measure the in situ room constant in favor of a more straightforward procedure. Instead of using GED measurements of the RDS and backing out the room constant using the Hopkins-Stryker equation, one can simply determine the approximate average absorption of the room using the procedure outlined in ISO 3746 A.3.2.1.[17] This method requires the mean absorption coefficient to be referenced from a table of descriptions, with an absorption coefficient of 0.05 for empty concrete or tile rooms, up to 0.5 for rooms with large amounts of sound-absorbing materials on ceiling and walls. The room constant is then determined using the surface area of the room and Eq. 2.11. Most of the research sponsor's mechanical test cells have an average absorption coefficient that ranges from 0.3 to 0.4. It should be noted that previously the room constant was calculated as a function of frequency, but by this simplified calculation, the room constant does not vary with frequency, eliminating the artifacts that caused the spectral shape to diverge from expected values.

Instead of using the two-point method procedure of using a system of equations with two instances of the Hopkins-Stryker equation based on two measurements along a line and solving for the unknown engine power and directivity factor, this simplified method uses one or more GED measurements that are averaged together, and a single instance of the Hopkins-Stryker equation is used to calculate the sound power. This, however, leaves one equation and two unknowns, the sound power of the engine, and the directivity factor of the engine.

The true directivity factor of the engine is significantly more complex than the theoretical models available and experimentally measuring the directivity factor of large engines is not logistically feasible. Although modifications to the direct term were investigated using expressions for the theoretical directivity factor of a baffled circular piston, a simply-supported vibrating plate, and a line source of finite length, none of these yielded results that were anywhere near expected values. Instead, the simplifying assumption of $\gamma = 1$ is applied, which is characteristic of an omnidirectional source. It is understood that the engine does not radiate omnidirectionally, but this significantly reduced the error introduced by the non-physical results in the directivity factor from the two-point method. Thus, the expression for sound power for the simplified GED method becomes:

$$\langle \Pi_{DUT} \rangle_t = \frac{2\langle w_{G,\beta} \rangle_{t,s} c}{\left(\frac{1}{4\pi r^2} + \frac{4}{R}\right)}. \tag{5.1}$$

Since the errors introduced by the direct term are likely due to the difficulty in achieving direct far field conditions, only measurement points away from the source in the predominantly reverberant field should be used. This will allow the reverberant term to dominate, which increases the probability of an accurate result.

5.2 The Simplified GED Method: Procedure

The procedure for the simplified GED method is as follows:

1. **Define Predetermined Variables**

   Document the length, width, and height of the test cell and multiply to obtain the room's volume. Also calculate the total surface area of the room. Do not subtract the volume or surface area of objects in the room from the total.

   Assign an average absorption coefficient to the room. This can be a relatively simple estimate, such as the method defined in ISO 3746 A.3.2.1. Most test cells with tile floor and perforated walls and ceilings fall in the 0.3 to 0.4 range. Once the mean sound absorption has been found, the room constant can be calculated using Eq. (2.11).

2. **Measure GED with Engine Operating at Desired Conditions**

   Set up the energy density probe in the room at a distance of at least a quarter wavelength (of the lowest frequency of interest) from any walls or large pieces of equipment, but maintain at least two effective engine diameters distance from the nominal center of the engine under test. The effective engine diameter can be found by averaging the approximate length, width, and height of the engine. This measurement method is sensitive to sensor placement if located too close to the engine. The probe should also be roughly in the same height plane as the engine, so position the probe so that the distance to the ground is approximately that of the height of the engine center. Measurement positions near the corners of the room typically allow for these constraints to be met. Document the nominal distance from the engine center to the sensor. To minimize potential error due to sensor placement sensitivity, it is encouraged but not imperative to

select an additional measurement position, meeting the aforementioned criteria, elsewhere in the test cell and repeat measurements.

Once the engine has reached its steady state, take a 30 second average of the one-third-octave band auto spectrum for each of the six channels, as well as the cross spectrum of each of the 3 pairs of phase-matched microphones. Repeat for all desired engine operating conditions.

3. **Post Process Data**

    a. Import the auto and cross spectra from each measurement.
    b. Calculate potential and kinetic energy densities according to Eq. (3.1) and Eq. (3.2), respectively. Average multiple measurements (if any) together.
    c. Weight PED by a factor 0.25 and KED by a factor of 0.75 to obtain GED.
    d. Calculate and/or define the various constants such as sound speed, wavenumber, measurement distance, room constant, etc.
    e. Calculate the sound power according to Eq. (5.1).
    f. Apply A-weighting to the one-third-octave band sound power data.
    g. Plot one-third-octave band sound power data.

5.3 The Simplified GED Method: Results

The simplified GED method was used to estimate the sound power based on the GED data previously used in the two-point method experiments, including the wooden enclosure simulating an extended source in the small reverberation chamber and the industrial engine in the mechanical test cell.

5.3.1 Laboratory Experiment Results

The simplified GED method results for the wooden enclosure with the enclosed subwoofer are shown in Fig. 5.1. The two-point method result from Ch. 4 is also shown for comparison. The simplified GED method, while slightly underestimating the overall sound power, shows a significant improvement to the two-point method estimate, with an overall value within 1.3 dB of the ISO 3741 result.

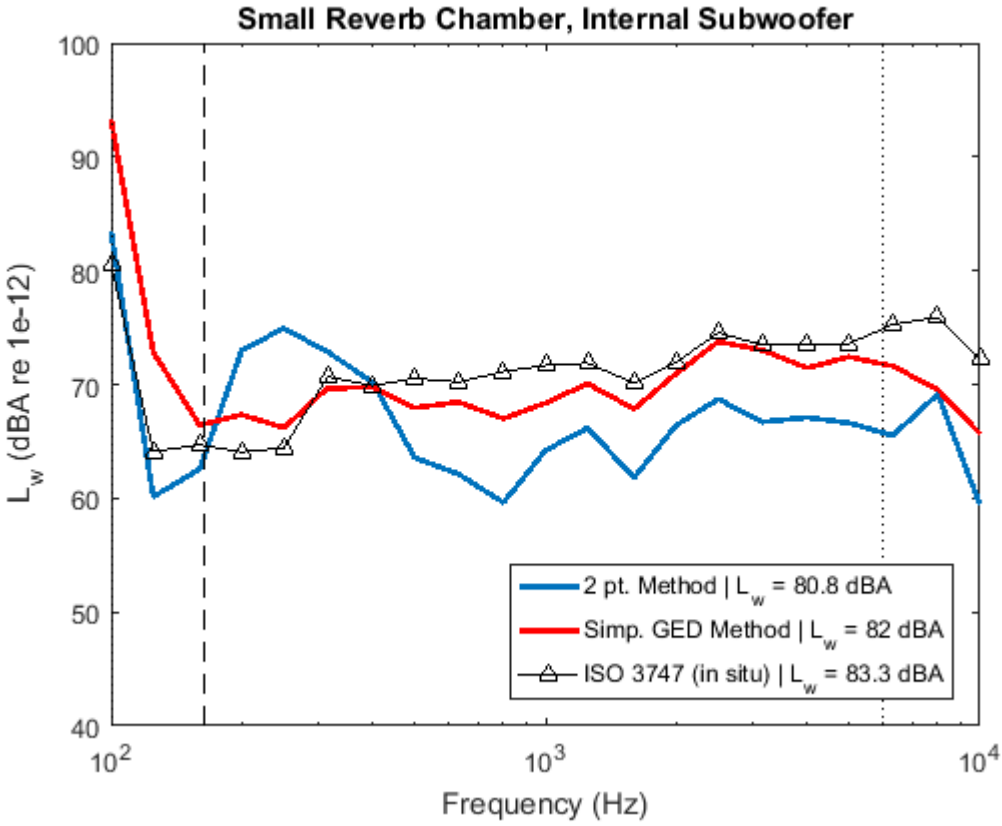

Fig 5.1. The sound power of the enclosure with a large subwoofer measured by the two-point method and simplified GED method with absorptive wedges present compared to the ISO 3741 result.

The simplified GED method was also applied to the laboratory experiment which included the shaker-driven panels and internal subwoofer acting as an extended source. When comparing the two-point method to the simplified GED method in this instance, as shown in Fig.

5.2, the simplified GED method again shows an improvement over the two-point method in its estimate of the sound power, with an overall estimate within 0.7 dB of the ISO 3741 result.

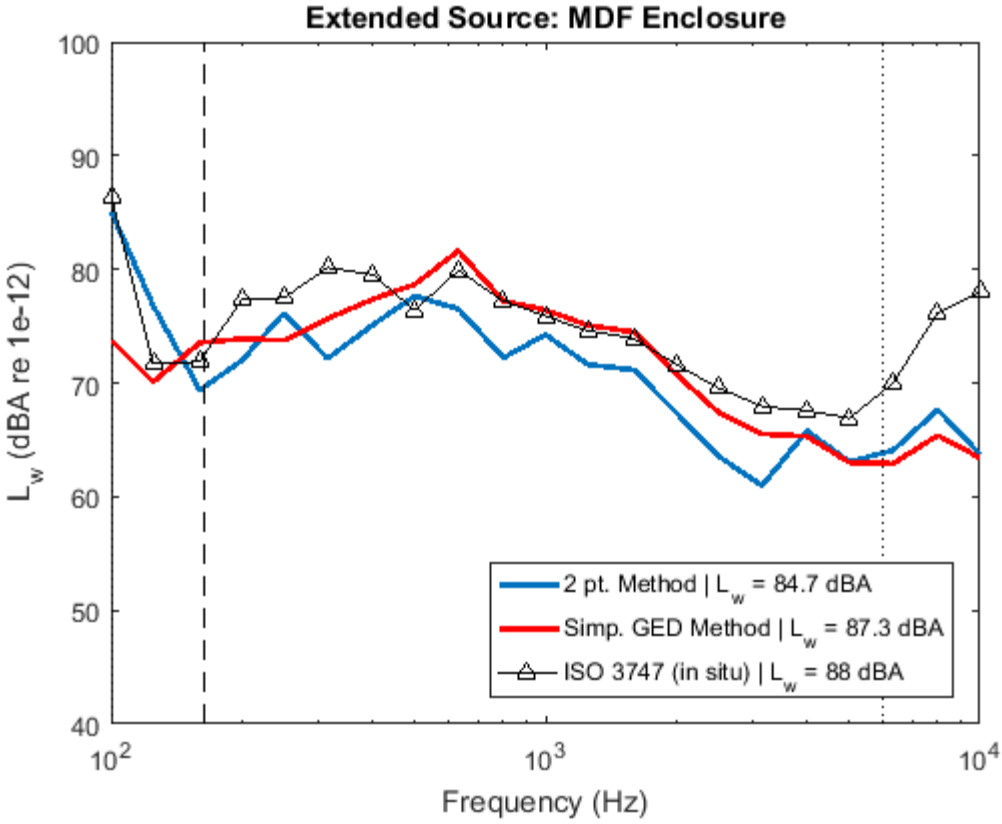

Fig 5.2. The sound power of the enclosure with thin panels, an enclosed subwoofer, and shakers rigidly attached to the enclosure walls measured by the simplified GED method and two-point method with absorptive wedges present compared to the ISO 3741 result.

While these laboratory results using the simplified GED method are not perfect estimations of the sound power relative to the ISO 3741 standard, they provide an improved result compared to the two-point method.

5.3.2 Engine Experiment Results

The sound power results calculated by the simplified GED method are shown below in Fig. 5.3. The two GED measurements with the greatest separation distance from the engine to the

probe were used. Various engine operating conditions are shown which have differing RPM and torque loads. Such as in Chapter 4, the sound power level is calculated to arbitrary references to protect sensitive information.

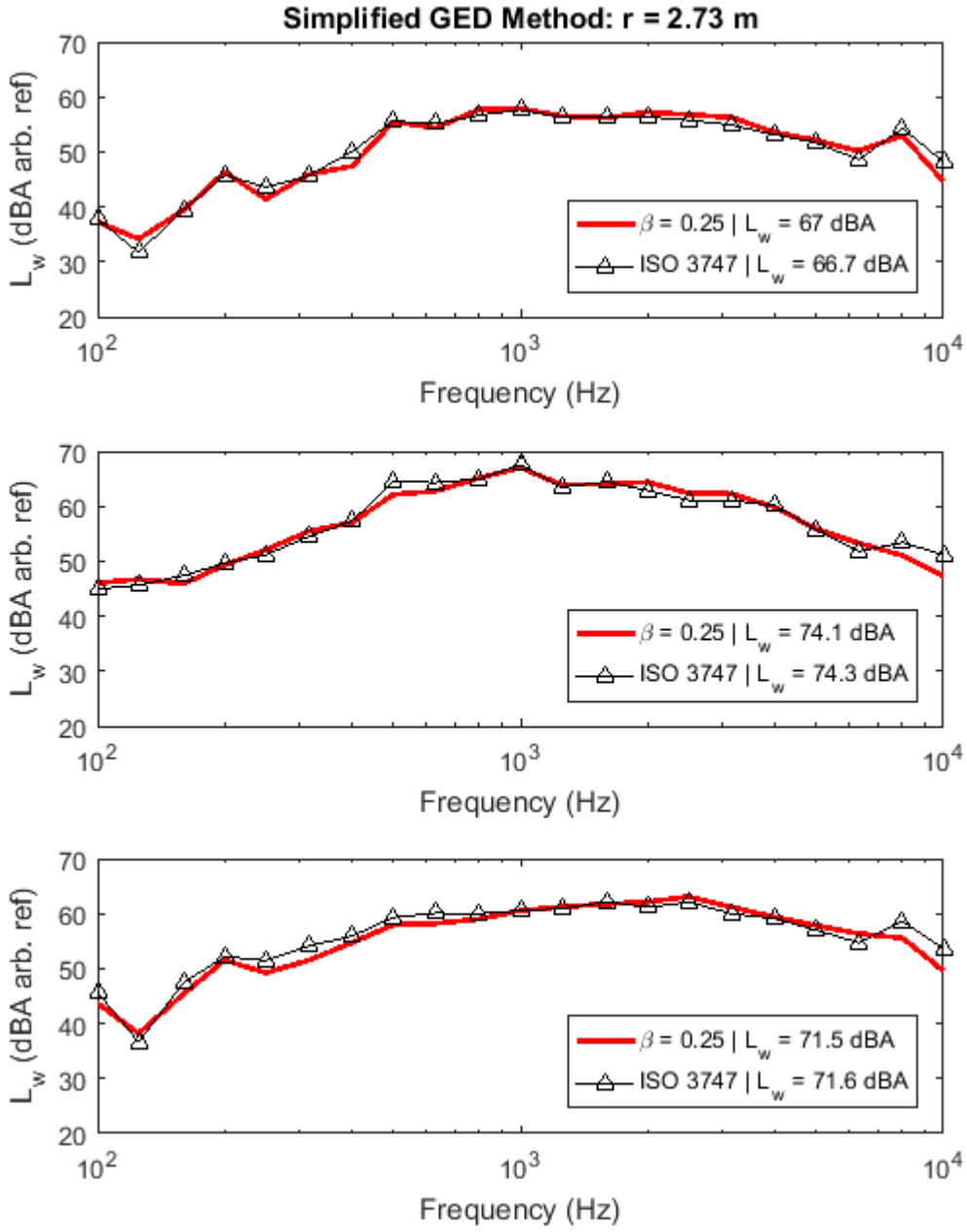

Fig 5.3. The sound power of the engine measured by the simplified GED method (red) and by ISO 3747 (black triangles) at a distance of 2.73 m from the engine center for three different operating conditions.

The results shown in Fig. 5.3 are from a single GED measurement position at 2.73 meters from the approximate engine center. Another GED measurement position at 3.4 meters was used in this study and the results are shown in Fig. 5.4 below.

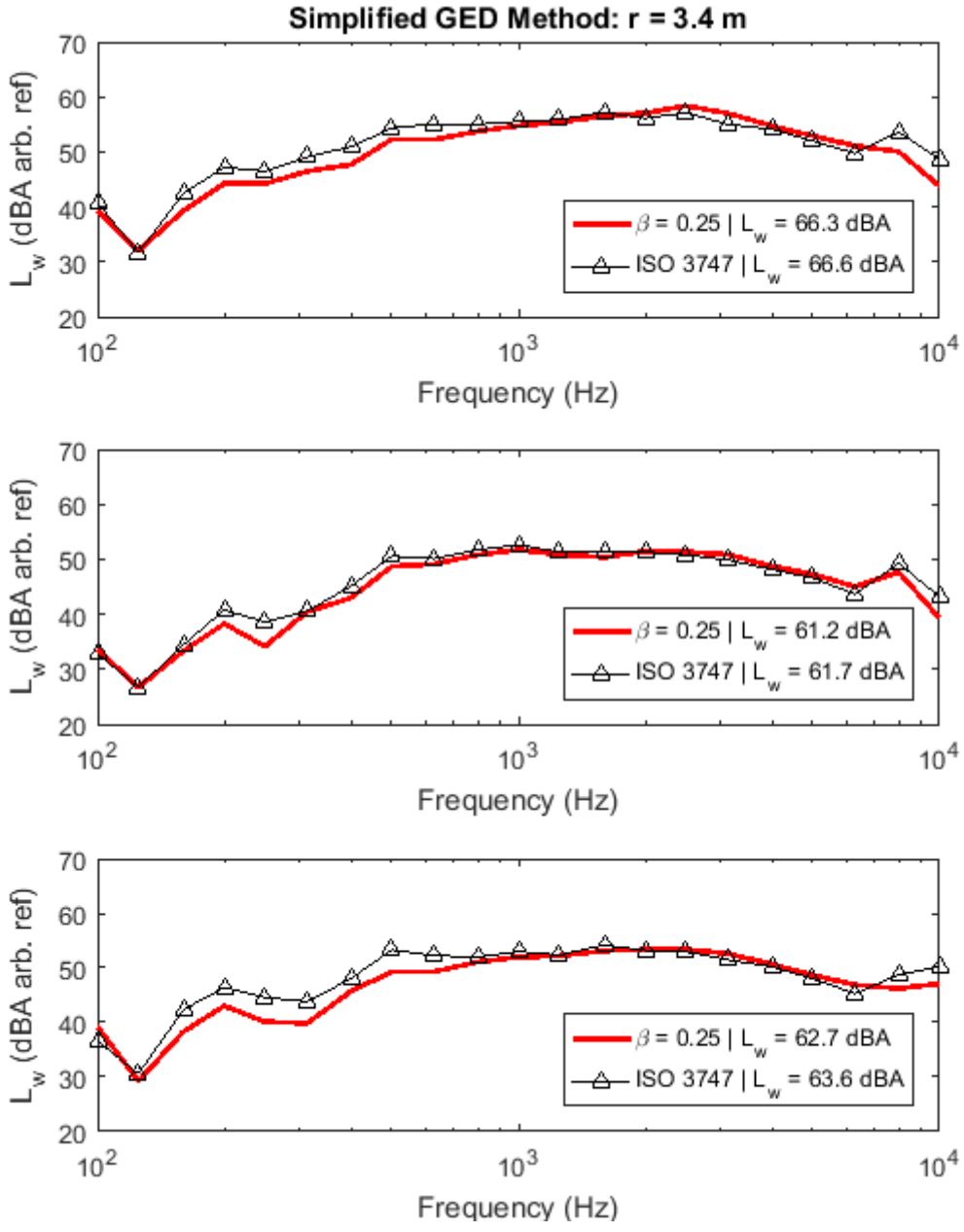

Fig 5.4. The sound power of the engine measured by the simplified GED method (red) and by ISO 3747 (black triangles) at a distance of 3.4 m from the engine center for three different operating conditions.

To test this method with a slightly larger data set, the engine measurements taken by Jensen in 2015 were included in this study, as shown in Fig. 5.5 and Fig. 5.6. Jensen's data include measurements of a different engine, but the test cell and experimental setup are roughly identical.

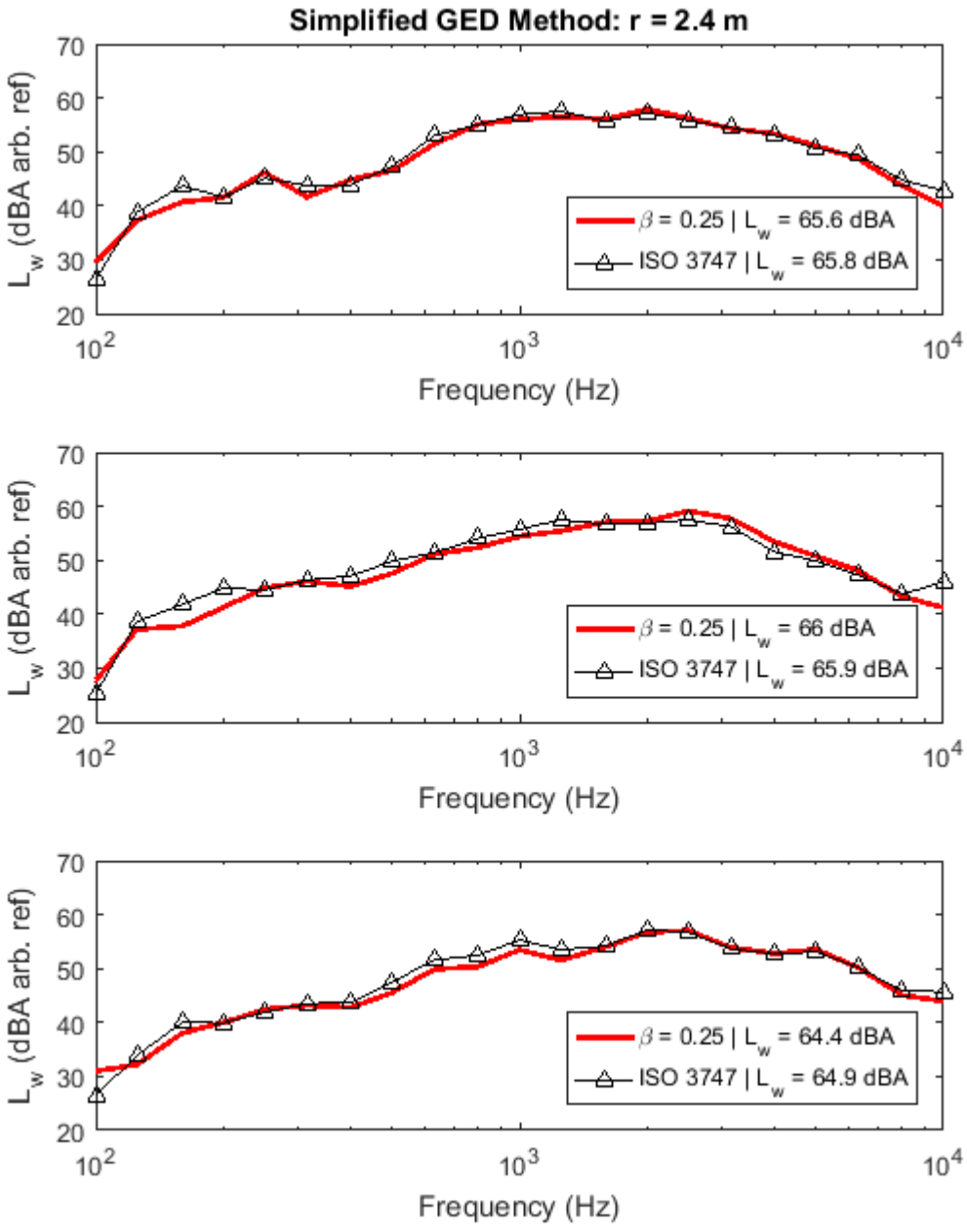

Fig 5.5. The sound power of the Jensen 2015 engine measured by the simplified GED method (red) and by ISO 3747 (black triangles) at a distance of 2.4 m from the engine center for three different operating conditions.

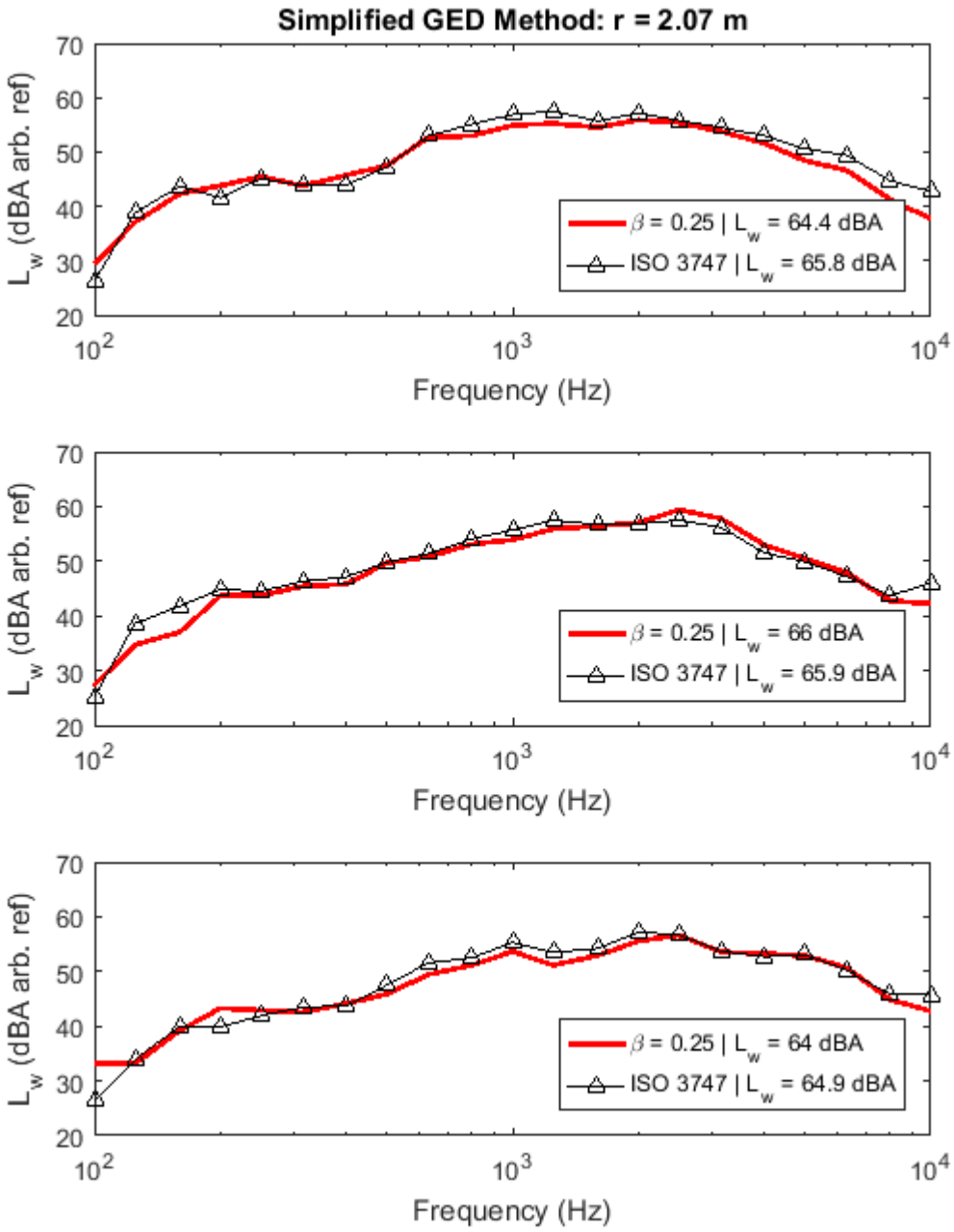

Fig 5.6. The sound power of the Jensen 2015 engine measured by the simplified GED method (red) and by ISO 3747 (black triangles) at a distance of 2.07 m from the engine center for three different operating conditions.

When measurements are taken at least two engine diameters away, results seem to converge nicely to the ISO 3747 results, often resulting in overall sound power levels within 1 dB of the

target ISO 3747 results. This was found to be the case for both data sets, those of Jensen and those conducted as a part of this work. These results suggest that the simplified GED method can be used to estimate the sound power of large industrial sources within mechanical test cells to survey-grade accuracy.

5.4 The Simplified GED Method: Limitations

Since it has been shown that the Hopkins-Stryker equation does not sufficiently describe the relationship between energy density and sound power when in the near field of an extended source, this method underestimates the sound power if the GED field is sampled too close to the engine. Examples of this are shown below in Fig. 5.7.

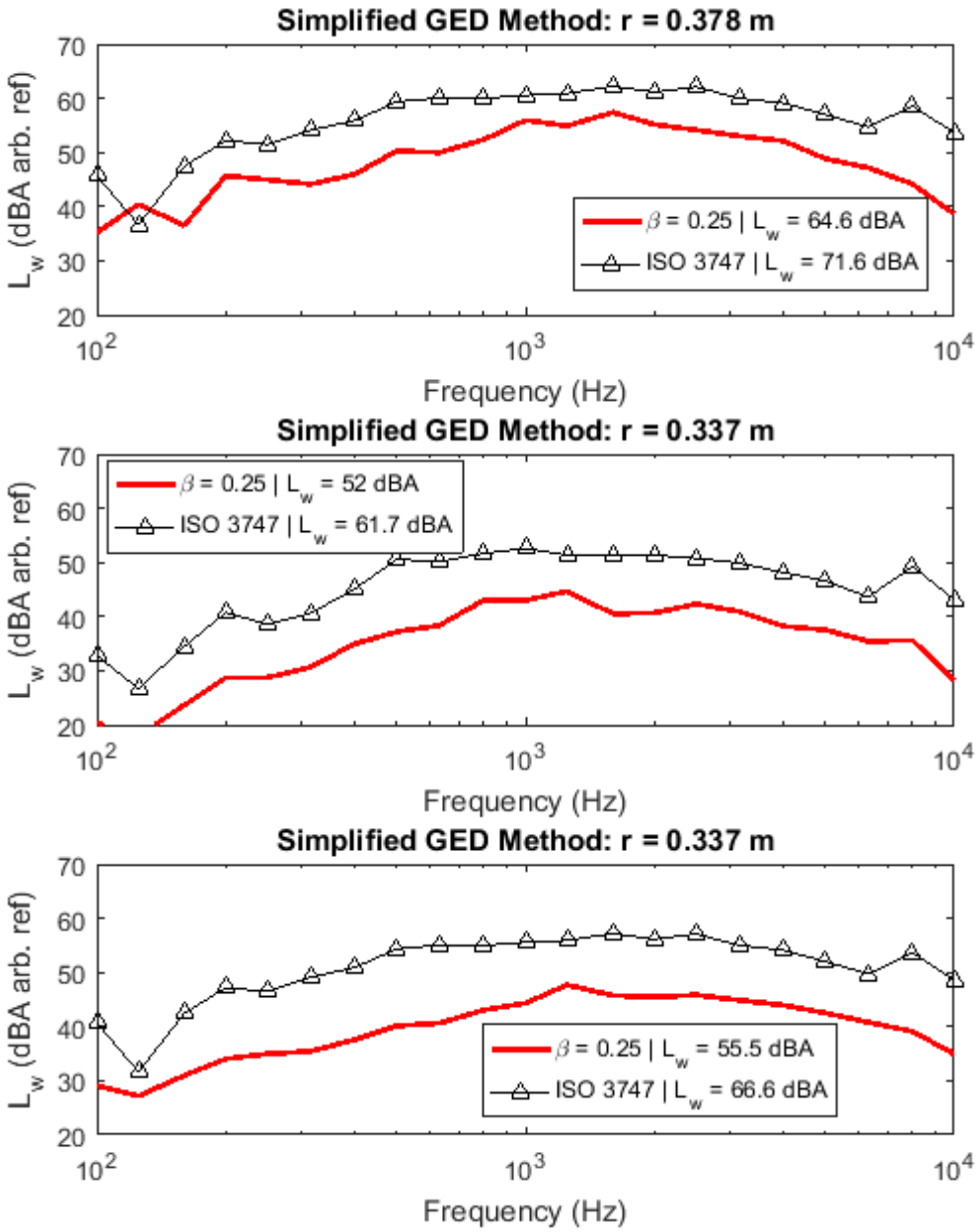

Fig 5.7. The sound power of the engine measured by the simplified GED method (red) and by ISO 3747 (black triangles) at a distance of approximately 0.35 m from the engine center for three different operating conditions.

When measurements are taken near the engine, results tend to underestimate the sound power by 6 to 11 dB. This exceeds, by a large margin, the expectations of a survey-grade measurement that requires +/- 3 dB accuracy. However, when the distance requirements are

appropriately met, the reverberant term dominates the effect of the direct term, and the overall sound power results converge to the expected result.

The difficulties encountered in the near field are however easily avoided by satisfying the aforementioned criteria of sensor placement no less than two effective engine diameters from the source. The challenges related to the two-point method when applied to large, extended sources have been appropriately remedied with the implementation of the simplified GED method.

Chapter 6

Conclusions and Recommendations

6.1 Conclusions

The two-point method has proven to be an efficient and pragmatic method for measuring the room constant and sound power of a compact source in semi-reverberant environments. When compared to current ISO standard measurements for sound power, the two-point method sound power estimates fall within 1 to 3 dB from the ISO results, depending on the measurement environment. However, the method underestimates the sound power when applied to large, extended sources whose radiation is not well described by the simple-source assumption.

This work has explored modifications to the two-point method to provide an efficient and accurate measurement method to assess the sound power of extended sources in semi-reverberant mechanical test cells. The findings of Marquez and Jensen were studied thoroughly and built upon in this work. Ultimately, the method was simplified considerably and improvements to the optimal sensor placement were incorporated to propose a new simplified GED method that is

more efficient than the two-point method. It has been shown experimentally to accurately estimate the sound power of large industrial engines to survey-grade accuracy.

Several insights were gained from this work and are summarized here:

1. The two-point method appropriately estimates the sound power of distributed compact sources in semi-reverberant environments. Experiments in a small reverberation chamber showed that the composite sound power of various sources was matched to ISO sound power measurements, so long as each of the sources was compact in nature. Only when sources became large and extended did the results begin to diverge.
2. As Jensen explored in detail in his work, the measurement of the room constant is critical and can have a profound influence on results. Spatial averaging improves this result, but often at the expense of experimental simplicity. It was discovered that a simple estimate of the room constant using nominal tabulated values of absorption coefficients was sufficient to obtain a meaningful room constant.
3. The direct term in the Hopkins-Stryker equation relies on the assumption of measurement in the direct far field and does not appropriately describe the direct energy density in the near field of sources. When sources are large, complex, and extended, this artifact becomes apparent since only the near field is accessible when in rooms that are only marginally larger than the source.
4. The directivity factor that the Hopkins-Stryker equation yields during the two-point method calculation for large industrial engines is often not physically reasonable. This nonphysical result was then used in the final calculation of sound power,

contributing to the considerable underestimation seen in the data taken by Jensen and as a part of this work. After exploring several modifications to the direct term based on theoretical directivity factors with no significant improvement, the simplifying assumption of $\gamma = 1$ was applied. The sound power results improved significantly, to the point of matching ISO sound power measurements for sensor positions located in the predominantly reverberant field.

5. The simplified GED method was tested experimentally and has been used to process data acquired previously by Jensen data to estimate the sound power of industrial engines to within 1.5 dB of ISO sound power measurements. When measurements are made at least two effective engine diameters from the center of the source, the GED, in combination with the simplifying assumptions discussed previously, allows for survey-grade accuracy sound power measurements of engines in mechanical test cells.

6.2 Recommendations for Future Work

Future work should include the acquisition of additional data on large industrial sources in various acoustical environments to further test the robustness of this method. The sponsor is currently making arrangements to replicate the experiments on other engines. Since the simplified GED method was developed long after measurements had taken place, it is poorly understood at what distances from the engine the sensor may be placed. There were essentially two “close” measurements and two “far” measurements, and the method works well for the

sensor positions far from the engine. Future work may look to better determine the optimal sensor placement.

Theoretical developments surrounding the direct term in near-field conditions could also be investigated to see if there are modifications that can be readily implemented to modify the Hopkins-Stryker equation to appropriately handle the violated assumptions that result in the underestimation of sound power, allowing the unabridged two-point method to achieve engineering-grade accuracy on large, extended sources. While Jensen incorporated the near-field correction term (based on a monopole) which improved near-field performance in close proximity to very compact sources, this did not scale well to larger sources. A possible correction term that is derived for large, extended sources could allow for the two-point method or simplified GED method to be used with greater versatility.

References

[1]ISO 3741:2010. "Acoustics – Determination of sound power levels and sound energy levels of noise sources using sound pressure – Precision methods for reverberation test rooms" (International Organization for Standardization, Geneva, 2010).

[2]ISO 3745:2012. "Acoustics – Determination of sound power levels and sound energy levels of noise sources using sound pressure – Precision methods for anechoic rooms and hemianechoic rooms" (International Organization for Standardization, Geneva, 2012).

[3]ISO 3744:2010. "Acoustics – Determination of sound power levels and sound energy levels of noise sources using sound pressure – Engineering methods for an essentially free field over a reflecting plane" (International Organization for Standardization, Geneva, 2010).

[4]Bodon, K Joshua, "Development, Evaluation, and Validation of a High-Resolution Directivity Measurement System for Played Musical Instruments," M.S. Thesis, Brigham Young University, 2016, available online at https://scholarsarchive.byu.edu/etd/5653/ (last viewed May 4, 2019).

[5]H. F. Hopkins and N. R. Stryker, "A proposed loudness-efficiency rating for loudspeakers and the determination of system power requirements for enclosures," Proc. IRE **36**, 315-335 (1948).

[6]B. Xu, S. D. Sommerfeldt, and T. W. Leishman, "Generalized acoustic energy density," J. Acoust. Soc. Am. **130**, 1370-1380 (2011).

[7]D. Marquez, "Estimating the Acoustic Power of Sources in Nonideal Enclosures Using Generalized Acoustic Energy Density," M.S. Thesis, Brigham Young University, 2014, available online at http://scholarsarchive.byu.edu/etd/3977/ (last viewed May 4, 2019).

[8]Z. Jensen, "Improvements to the Two-Point In Situ Method for Measurement of the Room Constant and Sound Power in Semi-Reverberant Rooms," M.S. Thesis, Brigham Young University, 2016, available online at http://scholarsarchive.byu.edu/etd/5724/ (last viewed May 6, 2019).

[9]C. Ianniello, "Walk away method versus reverberation time method in determining the room constant," Applied Acoustics **14**, 83-92 (1980).

[10]L. L. Beranek, *Acoustics* (McGraw-Hill, New York, 1954), pp. 109, 298-324.

[11]H. Kuttruff, *Room Acoustics*, 5th ed. (Spon Press, New York, 2009), pp. 44, 55, 83, 86, 131.

[12]M. Hodgson, "Experimental evaluation of the accuracy of the Sabine and Eyring theories in the case of non-low surface absorption,"J. Acoust. Soc. Am. **94**, 835-840 (1993).

[8]C. Ianniello, "Walk away method versus reverberation time method in determining the room constant," Applied Acoustics **14**, 83-92 (1980).

[9]R. Wells, "Apparatus noise measurement." Electrical Engineering **75**, 419-419 (1956).

[10]G. M. Diehl, *Machinery Acoustics*. (Wiley, 1974).

[11]ASTM Standard E33, 2010, "Standard Test Method for Field Measurement of Sound Power Level by the Two-Surface Method" (ASTM International, West Conshohocken, PA, 2010).

[12]P. G. Terrell, W. J. Hanson, and M. D. Ramsey, "Predicting noise reduction from absorptive treatments in industrial spaces: Alternatives to the 'Sabine' method," Am. Ind. Hyg. Assoc. J. **44**, 809-813 (1983).

[13] G.R.A.S. Sound & Vibration, "Vector Intensity Probe Type 50VI-1 Instruction Manual," available online at http://www.gras.dk/files/m/a/man_50VI-1.pdf (last viewed May 9, 2019).

[14]J.-C. Pascal, and J.-F. Li, "A systematic method to obtain 3D finite-difference formulations for acoustic intensity and other energy quantities," J. Sound and Vib. **310**, 1093-1111 (2008).

[15]ISO 354:2003. "Acoustics – Measurement of sound absorption in a reverberation room" (International Organization for Standardization, Geneva, 2003).

[16]Keele Jr, Don B, "What's so sacred about exponential horns?." Audio Engineering Society Convention **51**, 23 (Audio Engineering Society, 1975).

[17]ISO 3746:2010. "Acoustics – Determination of sound power levels and sound energy levels of noise sources using sound pressure – Survey method using an enveloping measurement surface over a reflecting plane" (International Organization for Standardization, Geneva, 2010).

Appendix A

Relevant Code

Two Point Method Code:

```
%% Four Point Method (2 Sources 2 measurement positions)
clear;
close all;


%load in the 3745 Sound Power File for reference directivity source
load('RDS_Directivity.mat')

Spcr = .025;
bmat = [0.25]; %[1 0 .5 .25]
fl = 100; fh = 6000;


%% Point to Files
FileName =
{'PT1_REF_CPB.Autospectrum.txt','PT1_REF_CPB.CrossSpectrum.txt','PT2_R
EF_CPB.Autospectrum.txt','PT2_REF_CPB.CrossSpectrum.txt'};
PathName = '';
FilterIndex = 1;

DataFlag = 0;
if FilterIndex == 0
return
elseif FilterIndex == 2
    DataFlag = 1;
elseif FilterIndex == 1
    DataFlag = 2;
end

 ISO3745FileNameref = 'ISO3745_SmallSpeaker_Lw 08-Jul-2015.mat';
 ISO3745PathNameref = '';
```

```
 ISO3745FilterIndexref = 1;

%% Weather
if ~exist('WFile')

    WFile = dir([PathName,'Weather.*x*']);

        WD = xlsread([PathName, WFile.name],'B1:B3');
        Tc = WD(1); % Celcius
        Pressure = WD(2); % mbar
        Hum = WD(3); % Hum (%)


    % rho0/c
    T0 = 293.15; %K
    RR = 287.058; % J/(kg*K)
    T = 273.15+Tc;

    rho = Pressure*100/(RR*T);
    c = 343.2*sqrt(T/T0); % cPierce = 331 + 0.6*Tc;

    %% T60
    T60File = dir([PathName,'T60.*x*']);

    if isempty(T60File)
        display('Need a T60 file in here (Name it T60.xlsx)')
        V = 1;
        S = 1;
        absorp = 0;
        R = 0;
        fsh = 0;
    else
        T60Data = xlsread([PathName, T60File.name]);

        T60f = T60Data(1,:).';
        T60  = T60Data(2,:).';

        Lx = T60Data(4,2);
        Ly = T60Data(5,2);
        Lz = T60Data(6,2);

        V = Lx*Ly*Lz;
        V_disp = 2.04 * 1.22 * 0.82;
        S = 2*Lx*Ly+2*Ly*Lz+2*Lz*Lx;

        V = V - V_disp;

        absorp = 1-exp(-(55.26*V)./(T60*c*S));
        R = S*absorp./(1-absorp);
```

```
        fsh = 2000*sqrt(mean(T60)./V);


    end

    %% Positions
    PosFile = dir([PathName,'Positions.*x*']);

    if isempty(PosFile)
        d = 0;
    else

        Positions = xlsread([PathName,PosFile.name]);

        rtot = (length(Positions)-2)/2;
        d = Positions(1,2);

    end



end

%% Load Reference Source Data

LFile = length(FileName);

switch DataFlag
    case 2
        cnt1 = 0;
        cnt2 = 0;
        for ii = 1:2:3
            RefPosInd(floor(ii/3)+1) = str2double(FileName{ii}(3));
            pl = 0;
            cnt1 = cnt1 + 1;
            for yy = 1:6
                fID = fopen([PathName,FileName{ii}]);
                Data = textscan(fID,'%f %f %f
%f','HeaderLines',yy*83+(yy-1)*pl);
                fc(1,:) = Data{:,2};
                G(cnt1,:,yy) = Data{:,3};
                pl = length(Data{:,3})+10;
                fclose(fID);
            end

            cnt2 = cnt2 + 1;
            pl = 0;
            for yy = 1:3
                fID = fopen([PathName,FileName{ii+1}]);
```

```
                Data = textscan(fID,'%f %f %f
%f','HeaderLines',yy*83+(yy-1)*pl);
                C(cnt2,:,yy) = Data{:,3}; % Real part of cross
spectrum
                pl = length(Data{:,3})+10;
                fclose(fID);

            end
        end
        kG = 2*pi*ones(size(G,1),1)*fc/c;
        kC = 2*pi*ones(size(C,1),1)*fc/c;
        PED = squeeze(G(:,:,1))/2/rho/c^2;

        Ep = 1./(24*rho*c^2)*sum(G,3)+1./(12*rho*c^2).*(sum(C,3));
        Ek = 1./(2*rho*c^2*kG.^2*Spcr^2).*sum(G,3) -
1./(rho*c^2*kC.^2*Spcr^2).*sum(C,3);
end

% PED = Ep;
KED = Ek;

%% Load in BG measurements

BGFileName = {'BG_CPB.Autospectrum.txt','BG_CPB.CrossSpectrum.txt'};
BGPathName = '';
BGFilterIndex = 1;


BGDataFlag = 0;
if BGFilterIndex == 0

elseif BGFilterIndex == 2
    BGDataFlag = 1;
elseif BGFilterIndex == 1
    BGDataFlag = 2;
end

%% Load BG Measurement Data
BGLFile = length(BGFileName);
clear Data G C
switch BGDataFlag
    case 2
        cnt1 = 0;
        cnt2 = 0;
        for ii = 1
            pl = 0;
            cnt1 = cnt1 + 1;
            for yy = 1:6
                fID = fopen([BGPathName,BGFileName{ii}]);
```

```
                Data = textscan(fID,'%f %f %f
%f','HeaderLines',yy*83+(yy-1)*pl);
                fc(1,:) = Data{:,2};
                G(cnt1,:,yy) = Data{:,3};
                pl = length(Data{:,3})+10;
                fclose(fID);
            end

            cnt2 = cnt2 + 1;
            pl = 0;
            for yy = 1:3
                fID = fopen([BGPathName,BGFileName{ii+1}]);
                Data = textscan(fID,'%f %f %f
%f','HeaderLines',yy*83+(yy-1)*pl);
                C(cnt2,:,yy) = Data{:,3}; % Real part of cross
spectrum
                pl = length(Data{:,3})+10;
                fclose(fID);

            end
        end
        kG = 2*pi*ones(size(G,1),1)*fc/c;
        kC = 2*pi*ones(size(C,1),1)*fc/c;
        PED = squeeze(G(:,:,1))/2/rho/c^2;
        BGEp = 1./(24*rho*c^2)*sum(G,3)+1./(12*rho*c^2).*(sum(C,3));
        BGEk = 1./(2*rho*c^2*kG.^2*Spcr^2).*sum(G,3) -
1./(rho*c^2*kC.^2*Spcr^2).*sum(C,3);
end

%% Solve for the room constant
cnt2 = 0;
for beta = bmat;
    cnt2 = cnt2 + 1;
    TED = 1/2*Ep + 1/2*KED;
    %     if beta == 1
    %         GED = PED;
    %     else
    GED = beta*Ep + (1-beta)*KED;
    BGGED = beta*BGEp + (1-beta)*BGEk;
    %     end
    ps = Pressure/10; %mbar to kPa
    ps0 = 101.325; % kPa
    theta = Tc; % celcius
    theta0 = 314; % Kelvin
    theta1 = 296; % Kelvin

    r_ref = [Positions(2+RefPosInd(1),1);
Positions(2+RefPosInd(2),1)];
```

```
     th_ref = Positions(2+RefPosInd(1),2);
     ph_ref = Positions(2+RefPosInd(1),3);


    alpha = absorption(theta,ps,Hum,fc);
    A0 = r_ref*alpha;
    delta = 10.^((A0.*(1.0053-0.0012.*A0).^1.6)/10);
    %delta = ones(size(delta)); %Override near-field correction

        [~,thIND] = min(abs(An.th-th_ref));
        [~,phIND] = min(abs(ph_ref-An.ph));
        Q = squeeze(An.Q(thIND,phIND,:)).';


    %     [Rinsitu(cnt2,:),W_ref(cnt2,:)] =
RcalcExp(2*GED(1,:),2*GED(2,:),r_ref(1),r_ref(2),Q,c,delta(1,:),delta(
2,:));
    [Rinsitu(cnt2,:),W_ref(cnt2,:)] =
RcalcExp_Corrected_BETA(2*GED(1,:),...

2*GED(2,:),r_ref(1),r_ref(2),beta,Q,c,fc,delta(1,:),delta(2,:));
    [BGRis(cnt2,:),BGW_ref(cnt2,:)] =
RcalcExp_Corrected_BETA(2*(GED(1,:)-BGGED),...
        2*(GED(2,:)-
BGGED),r_ref(1),r_ref(2),beta,Q,c,fc,delta(1,:),delta(2,:));

end

%%
figure  %Me tinkering
semilogx(fc,10*log10(BGRis),'-',T60f,10*log10(R'))
hold on
title('Room Constant')
xlabel('Frequency (Hz)')
ylabel('L_R')
legend('In-situ R (Two Point)','Est. R (From T60)','Est. R Adjusted')
hold off
xlim([10^2 10^4])
ylim([0 40])

%% Load in DUT measurements

FileName =
{'PT3_DUT_CPB.Autospectrum.txt','PT3_DUT_CPB.CrossSpectrum.txt','PT4_D
UT_CPB.Autospectrum.txt','PT4_DUT_CPB.CrossSpectrum.txt'};
PathName = '';
FilterIndex = 1;

DataFlag = 0;
```

```
if FilterIndex == 0
elseif FilterIndex == 2
    DataFlag = 1;
elseif FilterIndex == 1
    DataFlag = 2;
end

if ~exist('ISO3745FileName')
    ISO3745FilterIndex = 0;
    if ~ISO3745FilterIndex
        ISO3745Flag = 0;
    else
        ISO3745Flag = 1;
        load([ISO3745PathName,ISO3745FileName]);
    end
end

if ~exist('ISO3741FileName')

    ISO3741FileName = 'ISO3741_Lw_Both.mat';
    ISO3741PathName = '';
    ISO3741FilterIndex = 1;

    if ~ISO3741FilterIndex
        ISO3741Flag = 0;
    else
        ISO3741Flag = 1;
        load([ISO3741PathName,ISO3741FileName]);
    end

end

%% Load DUT Measurement Data
LFile = length(FileName);

switch DataFlag

    case 2
        cnt1 = 0;
        cnt2 = 0;
        for ii = 1:2:3
            DutPosInd(floor(ii/3)+1) = str2double(FileName{ii}(3));
            pl = 0;
            cnt1 = cnt1 + 1;
            for yy = 1:6
                fID = fopen([PathName,FileName{ii}]);
                Data = textscan(fID,'%f %f %f
%f','HeaderLines',yy*83+(yy-1)*pl);
                fc(1,:) = Data{:,2};
```

```
                G(cnt1,:,yy) = Data{:,3};
                pl = length(Data{:,3})+10;
                fclose(fID);
            end

            cnt2 = cnt2 + 1;
            pl = 0;
            for yy = 1:3
                fID = fopen([PathName,FileName{ii+1}]);
                Data = textscan(fID,'%f %f %f
%f','HeaderLines',yy*83+(yy-1)*pl);
                C(cnt2,:,yy) = Data{:,3}; % Real part of cross
spectrum
                pl = length(Data{:,3})+10;
                fclose(fID);

            end
        end
        kG = 2*pi*ones(size(G,1),1)*fc/c;
        kC = 2*pi*ones(size(C,1),1)*fc/c;
        PED = squeeze(G(:,:,1))/2/rho/c^2;
        Ep_dut = 1./(24*rho*c^2)*sum(G,3)+1./(12*rho*c^2).*(sum(C,3));
        Ek_dut = 1./(2*rho*c^2*kG.^2*Spcr^2).*sum(G,3) -
1./(rho*c^2*kC.^2*Spcr^2).*sum(C,3);
end

% PED = Ep_dut;
KED = Ek_dut;

%% Solve for the sound power and directivity of the DUT
cnt2 = 0;
for beta = bmat;
    cnt2 = cnt2 + 1;
    TED = Ep_dut + KED;
    %     if beta == 1
    %         GED = PED
    %     else
    GED = beta*Ep_dut + (1-beta)*KED;
    %     end

    ps = Pressure/10; %mbar to kPa
    ps0 = 101.325; % kPa
    theta = Tc; % celcius
    theta0 = 314; % Kelvin
    theta1 = 296; % Kelvin

    r_dut = [Positions(rtot+2+DutPosInd(1),1);
Positions(rtot+2+DutPosInd(2),1)];
```

```
    alpha = absorption(theta,ps,Hum,fc);
    A0 = r_dut*alpha;
    delta = 10.^((A0.*(1.0053-0.0012.*A0).^1.6)/10);
    delta = ones(size(delta));
    cnt = 0;

    [Qdut(cnt2,:),Wdut(cnt2,:)] =
WcalcExp_Corrected_BETA(2*GED(1,:),2*GED(2,:),r_dut(1),r_dut(2),beta,R
insitu(cnt2,:),c,fc,delta(1,:),delta(2,:));

    [BGQdut(cnt2,:),BGWdut(cnt2,:)] =
WcalcExp_Corrected_BETA(2*(GED(1,:)-BGGED),2*(GED(2,:)-BGGED),...

r_dut(1),r_dut(2),beta,BGRis(cnt2,:),c,fc,delta(1,:),delta(2,:));

    [QdutMeasuredR(cnt2,:),WdutMeasuredR(cnt2,:)] =
WcalcExp_Corrected_BETA(2*GED(1,fc>=min(T60f)&fc<=max(T60f)),...

2*GED(2,fc>=min(T60f)&fc<=max(T60f)),r_dut(1),r_dut(2),beta,R.',c,fc(f
c>=min(T60f)&fc<=max(T60f)),...

delta(1,fc>=min(T60f)&fc<=max(T60f)),delta(2,fc>=min(T60f)&fc<=max(T60
f)));

    [BGQdutMeasuredR(cnt2,:),BGWdutMeasuredR(cnt2,:)] =
WcalcExp_Corrected_BETA(2*(GED(1,fc>=min(T60f)&fc<=max(T60f))-
BGGED(fc>=min(T60f)&fc<=max(T60f))),...
        2*(GED(2,fc>=min(T60f)&fc<=max(T60f))-
BGGED(fc>=min(T60f)&fc<=max(T60f))),r_dut(1),r_dut(2),beta,R.',c,fc(fc
>=min(T60f)&fc<=max(T60f)),...

delta(1,fc>=min(T60f)&fc<=max(T60f)),delta(2,fc>=min(T60f)&fc<=max(T60
f)));

end

Lw = 10*log10(abs(Wdut)/1e-12);
TotLw = 10*log10(sum(10.^(Lw(:,fc>=fl&fc<=fh)*0.1),2));

LwMeas = 10*log10(WdutMeasuredR/1e-12);
TotLwMeas = 10*log10(sum(10.^(LwMeas(:,T60f>=fl&T60f<=fh)*0.1),2));

BGLw = 10*log10(abs(BGWdut)/1e-12);
BGTotLw = 10*log10(sum(10.^(BGLw(:,fc>=fl&fc<=fh)*0.1),2));

BGLwMeas = 10*log10(BGWdutMeasuredR/1e-12);
BGTotLwMeas =
10*log10(sum(10.^(BGLwMeas(:,T60f>=fl&T60f<=fh)*0.1),2));
```

```
% A-weighting
% From Annex F.3 ISO 3741 (2010)
fA = [50 63 80 100 125 160 200 250 315 400 500 630 800 1000 1250 1600
...
    2000 2500 3150 4000 5000 6300 8000 10000];
Ck = [-30.2 -26.2 -22.5 -19.1 -16.1 -13.4 -10.9 -8.6 -6.6 -4.8 -3.2 -
1.9 ...
    -0.8 0.0 0.6 1.0 1.2 1.3 1.2 1.0 0.5 -0.1 -1.1 -2.5];

LwA = Lw(:,fc <= max(fA) & fc >= min(fA)) + ones(length(bmat),1)*Ck;
LwAMeas = LwMeas(:,T60f <= max(fA) & T60f >= min(fA)) +
ones(length(bmat),1)*Ck(fA <= max(T60f) & min(T60f) <= fA);

TotLwA = 10*log10(sum(10.^(LwA(:,fA>=fl&fA<=fh)*0.1),2));
TotLwAMeas = 10*log10(sum(10.^(LwAMeas(:,T60f>=fl&T60f<=fh)*0.1),2));

BGLwA = BGLw(:,fc <= max(fA) & fc >= min(fA)) +
ones(length(bmat),1)*Ck;
BGLwAMeas = BGLwMeas(:,T60f <= max(fA) & T60f >= min(fA)) +
ones(length(bmat),1)*Ck(fA <= max(T60f) & min(T60f) <= fA);

BGTotLwA = 10*log10(sum(10.^(BGLwA(:,fA>=fl&fA<=fh)*0.1),2));
BGTotLwAMeas =
10*log10(sum(10.^(BGLwAMeas(:,T60f>=fl&T60f<=fh)*0.1),2));


%%
%%% A-weighted Plots %%%
figure
semilogx(fA,LwA,'linewidth',2)
hold on
legendStr = '';
for kk = 1:length(bmat)
    legendStr = [legendStr;{['\beta = ' num2str(bmat(kk)) ' | L_w = '
num2str(round(TotLwA(kk)*10)/10) ' dBA']}];
end

load('ISO3741_Lw_Both.mat') %update this one for comparison in the
plot

semilogx(Re.T60f,Re.LwA,'k-^')

legend(['\beta = 0.25 | L_w = '
num2str(round(10*log10(sum(10.^(LwA(fA>=fsh & fA<=fh)*0.1)))*10)/10) '
dBA'],...
['ISO 3741 SRC (in situ) | L_w = '
num2str(round(10*log10(sum(10.^(Re.LwA(Re.T60f>=fsh &
Re.T60f<=fh)*0.1)))*10)/10) ' dBA'],'AutoUpdate','off')
line([fsh fsh],[0 200],'color','k','linestyle','--')
```

```
line([fl fl],[0 200],'color','k','linestyle',':')
line([fh fh],[0 200],'color','k','linestyle',':')
xlim([100 10000])
ylim([40 100])
xlabel('Frequency (Hz)')
ylabel('L_w (dBA re 1e-12)')

title('Small Reverb Chamber, Shaker-driven Panels')

hold off

%%

rcrit = sqrt((mean(Qdut)*mean(Rinsitu))/(16*pi));
```

Two-Point Method Functions

```
function [Q,W] =
WcalcExp_Corrected_BETA(w1,w2,r1,r2,BETA,R,c,f,delta1,delta2)

k = 2*pi*f./c;

A1 = delta1.*(BETA + (1-BETA).*(1+1./((k.*r1).^2)));
A2 = delta2.*(BETA + (1-BETA).*(1+1./((k.*r2).^2)));

Q = abs(-(16*pi*r1.^2.*r2.^2.*(w1-w2))./(R.*(A2.*r1.^2.*w1-
A1.*r2.^2.*w2)));

W = w1./((Q./(4*pi*r1.^2*c).*A1 + 4./c./R));

% -((16 \[Pi] r1^2 r2^2 (wG1 - wG2))/(R (A2 r1^2 wG1 - A1 r2^2 wG2)))

function [R,W] =
RcalcExp_Corrected_BETA(w1,w2,r1,r2,BETA,Q,c,f,delta1,delta2)

k = 2*pi*f./c;

A1 = delta1.*(BETA + (1-BETA).*(1+1./((k.*r1).^2)));
A2 = delta2.*(BETA + (1-BETA).*(1+1./((k.*r2).^2)));

R = abs(-(16*pi*r1.^2.*r2.^2.*(w1-w2))./(Q.*(A2.*r1.^2.*w1-
A1.*r2.^2.*w2)));

W = w1./((Q./(4*pi*r1.^2*c).*A1 + 4./c./R));

% -((16 \[Pi] r1^2 r2^2 (wG1 - wG2))/(Q (A2 r1^2 wG1 - A1 r2^2 wG2)))
```

Simplified GED Method Code

```
%% Simplified Method for Sound Power Measurements using GED
%This code is to be used to calculate the A-weighted sound power using
GED
%measurements.
%User input required:
%Room Dimensions and average absorption coefficient
%ISO Standard Sound Power Measurements for comparison
%GED Measurement as a 31 element, one-third-octave band array. (20 Hz
to 20
%kHz)
%Distance from source and ED sensor.
clear;
close all;

c = 343; % sound speed, can define in terms of ambient conditions
fl = 100; fh = 10000; %Define frequencies of interest
fc =
[20,25,31.5,40,50,63,80,100,125,160,200,250,315,400,500,630,800,1000,.
..

1250,1600,2000,2500,3150,4000,5000,6300,8000,10000,12500,16000,20000];

%ISO Data
load('ISO3747.mat')
Re.T60f = ISOLwA.ISO_f; %Load in 3747 Data for comparison
ISO3747 = ISOLwA.LwA_Full;

%Room Dimensions
Lx = 5.48;
Ly = 7.01;
Lz = 4.575;

V = Lx*Ly*Lz; % Volume
S = 2*Lx*Ly+2*Ly*Lz+2*Lz*Lx; %Surface Area
alpha = 0.35; %Based on table lookup and room characteristics
T60 = 0.161*V/(-S*log(1-alpha)); %Calculate T60
fsh = 2000*sqrt(mean(T60)./V); %Calculate Schroeder Frequency

%GED Data
r_dut = 2.63; %distance from engine center to field point
load('GED.mat') %Load in GED measurement

fA = [50 63 80 100 125 160 200 250 315 400 500 630 800 1000 1250 1600
...
    2000 2500 3150 4000 5000 6300 8000 10000];

Qadm.alpha = alpha;
```

```
Qadm.R = (-S*log(1-Qadm.alpha))/(1-Qadm.alpha);
Qadm.Q = 1;
Qadm.r = r_dut; %approximate offset between edge of engine and center
Qadm.ISO3747 = ISO3747;
Qadm.ISO3747tot = ISOLwA.TotLwA.Full;
Qadm.fA = fA;
Qadm.fISO = ISOLwA.ISO_f;


for n=1:length(GED)
Qadm.Wdut(n) = (2.*GED(1,n)*c)./((Qadm.Q/(4*pi*Qadm.r^2))+(4/Qadm.R));
Qadm.Lw(n) = 10*log10(abs(Qadm.Wdut(n))/1e-12);
end

%A-Weighting the result
Ck = [-30.2 -26.2 -22.5 -19.1 -16.1 -13.4 -10.9 -8.6 -6.6 -4.8 -3.2 -
1.9 ...
    -0.8 0.0 0.6 1.0 1.2 1.3 1.2 1.0 0.5 -0.1 -1.1 -2.5];

Qadm.LwA = Qadm.Lw(:,fc <= max(fA) & fc >= min(fA)) + ones(1,1)*Ck;

%% Figure
figure
semilogx(fA,Qadm.LwA,'r','linewidth', 2)
hold on
semilogx(ISOLwA.ISO_f,ISO3747,'k-^')
hold off

legend(['L_w = ' num2str(round(10*log10(sum(10.^(Qadm.LwA...
    (fA>=fsh & fA<=fh)*0.1)))*10)/10) ' dBA'],...
    ['ISO 3747 | L_w = ' num2str(round(Qadm.ISO3747tot,1)) ' dBA']...
    ,'location','SE')

xlim([100 10000])
ylim([70 120])
xlabel('Frequency (Hz)')
ylabel('L_w (dBA re 1e-12)')

title(['Simplified GED Method r = ' num2str(Qadm.r) ' m'])
```